Particles and Their Properties

Review of Particle Properties Physics Letters 33B, No. 1 (1970)

SELECTED TOPICS IN THE THEORY OF ELECTROMAGNETIC INTERACTIONS

S.B. Gerasimov

Laboratory of Theoretical Physics,
Joint Institute for Nuclear Research,
Dubna, USSR.

I. INTRODUCTION.

In the present lectures we shall discuss a few selected topics in the theory of electromagnetic (e.m.) interactions. It was intention of the author to select for discussion the questions, that would be of current interest, and to stress, whenever possible, the consequences of such remarkable features of the e.m. interactions as the gauge invariance (or divergence condition) and smallness of the universal coupling constant ($\alpha = \frac{e^2}{4\pi} = \frac{1}{137}$). Considering only the terms of the lowest order in α , we have the unique possibility to study the dependence of the cross sections on the invariant mass of the virtual photon in elastic and inelastic lepton scattering (the spacelike region of $q^2 < 0$) and in annihilation and creation of the lepton pairs (the time-like region $q^2 > 0$). The study of the q^2 - dependence of the e.m. current matrix elements will be the central and pivotal line, which unite all the questions to be considered. The contents of the separate sections of these notes can be outlined as follows. In Section 2 we shall deal with the e.m. interactions of leptons and some results of the experimental check of QED at "large" ($q \to 0$) and "small" ($q \to \infty$) distances are briefly reviewed. The rest will be devoted to the e.m. interactions of hadrons. In the interval $-\infty < q^2 < +\infty$ two points: $q^2 = 0$ and

$q^2 = m_v^2$ ($v = \rho^0, \omega, \varphi$) are of special interest for the reasons, which are selfevident. In Section 3 the case of $q^2 = 0$ and $q \to 0$ is considered. The exact low energy theorems for emission and absorption of the soft quanta are shown to follow from the gauge and relativistic invariance of the theory. Dispersion sum rules for the photoabsorption cross sections are derived and some consequences from them are discussed. Section 4 deals with the region $0 \leq q^2 \leq m_v^2$ and $\frac{m_v^2}{2q} \to 0$, which is the region most suitable for the application of the vector meson dominance model of e.m. interaction of hadrons. The experimental data and the theoretical implications on elastic and inelastic electron-nucleon scattering are discussed in Section 5. In Section 6 we turn to the time-like $q^2 > 0$, to consider both the annihilation and creation of lepton pairs in the reactions, where hadrons are participating.

2. GAUGE INVARIANCE AND TESTS OF QED.

2.I Basic Equations

It is well - known to everyone, that the lepton quantum electrodynamics (QED) is based on the simplest form of the Lagrangian, which describes the evolution of coupled system of two fields: the spinor field $\psi(x)$ of leptons and the vector field $A_\mu(x)$ of photons:

$$\mathcal{L}_{tot}(\bar{\psi}, \psi, A) = \mathcal{L}_e(\bar{\psi}, \psi) + \mathcal{L}_\gamma(A) + \mathcal{L}_{int}(\bar{\psi}, \psi, A) \qquad (2.1)$$

The free e.m. field Lagrangian

$$\mathcal{L}_\gamma(A) = -\frac{1}{4} F_{\mu\nu}(x) F^{\mu\nu}(x) \qquad (2.2)$$

$$F_{\mu\nu} = \partial_\mu A_\nu - \partial_\nu A_\mu , \qquad \partial_\mu = \frac{\partial}{\partial x_\mu} ,$$

is invariant under substitution

$$A_\mu \longrightarrow A_\mu(x) - \partial_\mu f(x) \tag{2.3}$$

where f(x) is an arbitrary function.

In the free lepton field Lagrangian

$$\mathcal{L}_e = -\bar{\Psi}(x)(i\gamma_\mu \partial_\mu + m)\Psi(x) \tag{2.4}$$

we make now the substitution

$$\partial_\mu \rightarrow \partial_\mu + ie A_\mu \tag{2.5}$$

which leads to

$$\mathcal{L}_e(\bar{\Psi}, \Psi) \longrightarrow \mathcal{L}_e(\Psi) + \mathcal{L}_{int}(\bar{\Psi}, \Psi, A)$$

with

$$\mathcal{L}_{int} = e\bar{\Psi}\gamma_\mu \Psi A_\mu \equiv e j_\mu(x) A_\mu(x) \tag{2.6}$$

As a result, we have, that both the Lagrangian (I.I) and the field equations

$$\begin{aligned} &\Box A_\mu(x) - \partial_\mu \partial_\nu A_\nu(x) = -e j_\mu(x) \\ &(i\gamma^\mu \partial_\mu + m)\Psi(x) = e\gamma^\mu \Psi(x) A_\mu(x) \end{aligned} \tag{2.7}$$

are invariant under the gauge tranformations

$$\begin{aligned} &\Psi \rightarrow e^{ief(x)}\Psi(x), \quad \bar{\Psi}(x) \rightarrow \bar{\Psi}(x) e^{-ief(x)}, \\ &A_\mu(x) \longrightarrow A_\mu(x) - \partial_\mu f(x) \end{aligned} \tag{2.8}$$

i.e. gauge - invariant.

The lepton current conservation

$$\partial_\mu j_\mu(x) = 0 \tag{2.9}$$

follows automatically from the gauge - invariant Lagrangian.

2.2 Experimental Foundation of Gauge Invariance.

The gauge invariance is postulated as one of the basic symmetry principles of the e.m. interactions and it is the

mathematical formulation of two empirical facts of great importance:

I. The current conservation (I.9) or the electric charge conservation.

2. The masslessness of the photon i.e. the absence of the "mass term"

$$-\frac{m_\gamma^2}{2} A_\mu A^\mu \qquad (2.10)$$

in the Lagrangian $L_\gamma(A)$.

The best experimental evidence for the charge conservation is the absence of non-charge-conserving decays

$e^- \to 3\nu$ ($\tau_e > 2 \times 10^{21}$ yr) and $e^- \to \nu + \gamma$ ($\tau_e > 4 \times 10^{22}$ yr)[1]

The conserved electric charge is the universal coupling constant of the e.m. interaction. The confirmation of this universality consists in the precise determination of the charges of stable particles e, p, ν. It was shown[2] that the electron charge differs from that of proton by less than 5 parts in 10^{19} and that the neutron charge (hence, the neutrino charge from β-decay $n \to p + e + \nu$) is less than $10^{-19} \times |e|$, (e is the electron charge).

Table I gives the list of the upper bounds for the photon mass in units of the electron mass m_e (correspondingly, the lower bounds for the Compton wavelength $\lambda\!\!\!^{-}_\gamma$ of photon) which were obtained from various experiments.

T a b l e I

Summary of upper bounds for the photon mass (from Ref.3)

Method	λ_γ	m_γ / m_e
I) The dispersion of the velocity of light from the double stars.	0,I cm	$I0^{-9}$
2) Velocity of the radio waves.	I km	$I0^{-I5}$
3) The Coulomb low.	I0 km	$I0^{-I6}$
4) Magnetic field of the Earth.	30 000 km	$I0^{-20}$

A few short comments concerning Table I are worth to mention:

I. It is evident, that the velocity of a photon V would not be the universal constant ($v<c$), when $m_\gamma \neq 0$, but would be a function of the photon energy

$$\frac{V}{C} = \frac{k}{\sqrt{k^2+m_\gamma^2}} = \frac{1}{\sqrt{1+(\lambda/\lambda_\gamma)^2}}$$

(for instance, the velocity of the blue light would be higher than that of the red light). The light velocity dispersion in vacuum should cause the colour phenomena to be observed in the eclipse of the double stars.

2. As $m_\gamma \neq 0$ the Coulomb potential should be replaced by the Yukawa potential

$$\frac{1}{r} \rightarrow \frac{e^{-m_\gamma r}}{r} \qquad (2.II)$$

while the vector-potential of the magnetic dipole $\vec{\mu}$ is modified in the following manner

$$\frac{[\vec{\mu}\times\vec{r}]}{r^3} \longrightarrow \frac{[\vec{\mu}\times\vec{r}]}{r^3}(1+m_\gamma r)\frac{e^{-m_\gamma r}}{r} \qquad (2.12)$$

The best experimental limit for m_γ, reached up to now, is just coming from a comparison of Eq.(2.12) with the magnetic field of the Earth.

Henceforth, we shall assume that the gauge invariance is satisfied exactly.

2.3 Modifications of the theory and the high energy tests of QED.

The dynamical model specified by the Lagrangian(2.I) is very elegant and economical one. All observables are expressed finally in terms of the only universal coupling constant and the lepton masses, which are assumed to be given. The Lagrangian (2.I) is clearly to have meaning as an "effective" one, for it does not take into account the interactions of the Dirac and Maxwell field with other fields. Among the reasons for the possible breaking of "pure" leptonic QED is that the strong and weak interactions have eventually to display itself in electromagnetic effects. Another possible cause for disagreements between the theory and experiment could be the violation of fundamental principles underlying the present - day quantum field theory , such as the Lorentz invariance, the general principles of the quantum mechanical description (the probability conservation, to mention) and

the locality of interaction between the fields.

The locality is commonly suspected most of all, as it is responsible for mathematically meaningless divergent expressions which appear in theory. Qualitatively, these ultraviolet divergencies occur due to the following. Upon integrating over internal momenta in the Feynman graphs we are summing over all possible states of a system with the infinite degrees of freedom and the number of states grows with energy too rapidly to be compensated by decreasing of the transition probability to these states. An additional compensation needed to make the theory convergent is carried out artificially, by attaching the phenomenological form factors to the propagators and or vertices in the Feynman diagrams. In this section we discuss briefly the bounds, which gauge invariance condition put on various models of the "broken" QED.

The breaking of the QED consists usually in its "nonlocal" modification.[4] In particular, one can suppose that in the mutual transformations of the particles, such as $a \to b + c$ and $a + \bar{b} \to c$, all three particles are barred from the simultaneous localization in the same space-time point, and that the field operators, averaged over the space-time region of the characteristic dimension of l ("elementary length")

$$\varphi(x) = \Phi[x, F] = \int F(x - x') \Phi(x') dx' \qquad (2.13)$$

enter the interaction Lagrangian. In Eq.(2.13) $F = F(x)$ is the form factor. Non-locality, such as in Eq.(2.13), intro-

duces the additional momentum dependence in the matrix elements. Converting Eq.(2.I3) into the momentum representation one can obtain

$$\varphi(x) = \frac{1}{(2\pi)^4} \int d^4p\, e^{-ipx} \bar{F}(p)\, \bar{\Phi}(p) = \bar{F}(\hat{p})\, \Phi(x)\,, \qquad (2.I4)$$

where the bar denotes the Fourier transform of the function in question (for instance, $\bar{F}(\hat{p})$ is the Fourier tranform of $F(x)$), $\hat{p} = -i\partial_\mu$ is the momentum operator in the coordinate representation.

To maintain the gauge invariance the differential operators acting on the charged particle fields should appear only in the form of the following gauge - invariant combination

$$\hat{p}_\mu - e A_\mu(x)$$

Hence, if we are going to make use of the modified lepton fields

$$\Psi(x, F) = \bar{F}(\hat{p} - eA)\, \Psi(x) \qquad (2.I5)$$

we shall have in the interaction Lagrangian non-linear dependence of e.m. field $A_\mu(x)$, which leads to the presence of the multiphoton vertices and additional difficulties with divergencies in higher order diagrams will appear.

The commonly accepted parametrization of the matrix elements of the processes with the fermion propagator - the Bethe-Heitler pair production and the Bremsstrahlung -

$$\begin{aligned} &\gamma + A \to \ell^+ \ell^- + A \\ &\ell^\pm + A \to \ell^\pm + \gamma + A \end{aligned} \qquad (2.I6)$$

is of the form[5]

$$\frac{\sigma_{exp}}{\sigma_{th}} = 1 \pm \frac{m^4}{\Lambda^4} \qquad (2.17)$$

where $m = m_{e^+e^-}$ or $m_{e\gamma}$, is the invariant mass of the final state in Eq.(2.16), Λ is the cut-off momentum.

Theoretically, the model of the broken QED with the modified photon propagator

$$\frac{1}{K^2} \to \frac{1}{K^2} - \frac{1}{K^2-\Lambda^2} = \frac{\Lambda^2}{K^2(\Lambda^2-K^2)} \qquad (2.18)$$

looks more attractive as it can be made consistent with the absence of divergences, the gauge invariance and the unitarity of the S-matrix[4].

This model can be checked in the processes, including the virtual photon lines in the lowest order diagram:

$$e^- + e^- \to e^- + e^-$$
$$e^+ + e^- \to e^+ + e^-$$
$$e^+ + e^- \to \mu^+ + \mu^-$$

In Table 2 the summary is given of the values of Λ obtained from recent high energy tests of QED.[5]

T a b l e 2

Summary of recent high energy tests of QED.

Experiment	Value of Λ (95% Confidence Limit)
I. $e^- + e^- \to e^- + e^-$	
$m_{e^-e^-}$ = 1110 MeV	$\Lambda > 4$ GeV
2. $e^+e^- \to e^+e^-$	
$m_{e^+e^-}$ = 1020 MeV	$\Lambda > 2.6$ GeV

3. $e^+e^- \to \mu^+\mu^-$ $\quad \Lambda > 1{,}3$ GeV

$m_{e^+e^-} = 1020$ MeV

4. $\gamma + C \to C + e^+e^-$ $\quad \Lambda > 1.4$ GeV

$m_{e^+e^-} \leq 900$ MeV

5. $\gamma + C \to C + \mu^+\mu^-$ $\quad \Lambda > 1.5$ GeV

$m_{\mu^+\mu^-} \leq 1225$ MeV

6. $e^- + C \to C + e^- + \gamma$ $\quad \Lambda > 1.5$ GeV

$m_{e\gamma} \leq 1030$ MeV

7. $\mu^- + C \to C + \mu + \gamma$ $\quad \Lambda > 0.7$ GeV

$m_{\mu\gamma} \leq 650$ MeV

2.4 The low energy tests of QED.

We turn now to the experimental tests of the theoretical predictions for the static properties of a system: the bound state energies and the lepton magnetic moments.

Firstly, we shall discuss the hydrogen atom energy levels. As is well known, in the nonrelativistic approximation the bound state levels of the electron in the Coulomb field are degenerate with respect to the orbital angular momentum:

$$1s_{1/2}\ ;\quad 2s_{1/2}\ 2p_{1/2}\ 2p_{3/2}\ ;\quad 3s_{1/2}\ 3p_{1/2}\ 3p_{3/2}\ 3d_{3/2}\ 3d_{5/2}\ ;\ \ldots$$

(where each state is specified by the principle quantum number n, the orbital angular momentum $l = 0, 1, 2, \ldots n-1$, and the total angular momentum j).

If we use the Dirac equation instead of the Schroedinger one, then due to relativistic effects (mainly, due to the spin-orbit coupling) the term with fixed n is splitted

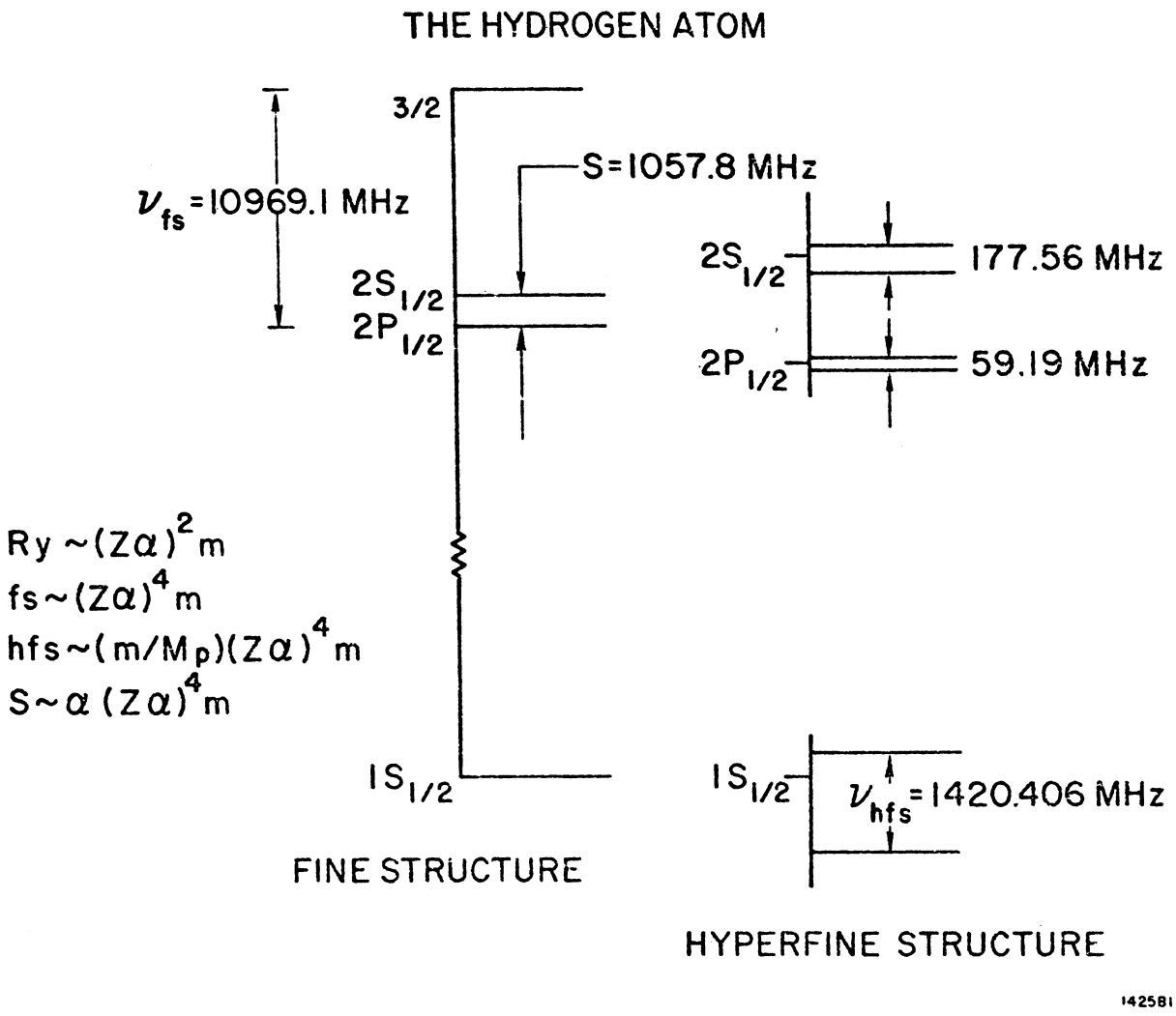

Fig. 1 The energy level structure of atomic hydrogen.

into n components of the fine structure. All of them have the same values of n and j but the different values of $l = j \pm 1/2$:

$$1s_{1/2}\ ;\quad 2s_{1/2}\ 2p_{1/2}\ ,\ 2p_{3/2}\ ;\quad 3s_{1/2}\ 3p_{1/2}\ ,\ 3p_{3/2}\ 3d_{3/2}\ ,\ 3d_{5/2}\ ;$$

At last, if the electron-proton relative motion is described in a completely relativistic manner by the two-particle Bethe-Salpeter equation and if the proton structure is taken into account in the form of a given static charge and magnetic moment distribution, then all levels are splitted, each level with a given j being splitted into two levels with $\mathcal{J} = j \pm 1/2$, where $\mathcal{J}$ is the total angular momentum of the electron-proton system. The last type of splitting forms the hyperfine structure of the hydrogen atom (see Fig.I).

We have not yet told anything about the modification of the effective electron-proton interaction due to the electron "structure" i.e. the higher QED corrections, corresponding to the Feynman graphs, presented in Fig.2.

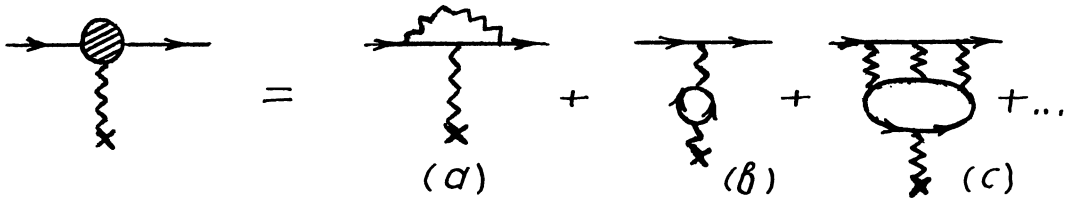

Fig. 2 Feynman diagrams representing the electron "structure".

The calculations of the radiative corrections to the bound state energies reveal the following features.

The values of the fine structure and hyperfine structure splittings

$$\Delta E_{fs} = E(n, \ell, j = \ell + 1/2) - E(n, \ell, j = \ell - 1/2) \qquad (2.19)$$

$$\Delta E_{hfs} = E(n, j, \mathcal{J} = j + 1/2) - E(n, j, \mathcal{J} = j - 1/2) \qquad (2.20)$$

are weakly dependent on the radiative corrections (they contribute about 0,1% = 1000 ppm)

It is important to note also, that among various terms the dominant contribution to Eqs.(2.19) and (2.20) comes from the interaction of the external e.m. field with an anomalous magnetic moment of electron (Fig.2(a)). All the other terms, but the electron anomalous moment correction, contribute to ΔE^{H}_{hfs} (n=1) about 60 ppm, to $\Delta E^{\mu^+e^-}_{hfs}$ (n=1) about 200 ppm and to ΔE^{H}_{fs} (n=2) 1,2 ppm, while the experimental errors are $\pm 1{,}2 \times 10^{-12}$, ± 9 ppm and ± 5 ppm, respectively.[6)]

The tremendous precision of ΔE^{H}_{hfs} (n=1) attained using the hydrogen maser technique cannot, unfortunately, be utilized as a check of QED until a better theoretical understanding of the nucleon polarization can be made.

The complications due to the strong interaction dynamics are absent in studying the hyperfine splitting of muonium (μ^+e^-). The main trouble here is that the electron/muon mass ratio is not known to sufficient precision.

Contrary to ΔE_{fs} and ΔE_{hfs} , the lepton magnetic moment anomalies and the Lamb shift

$$S = E(n, \ell = j + 1/2, j) - E(n, \ell = j - 1/2, j) \qquad (2.21)$$

are totally the higher order QED quantities.

The situation with the Lamb shift have caused the anxiety for a long time, because various experiments were in satisfactory agreement with each other but disagree strongly with a theory.[6] However, the recalculation of the α^2- corrections to the electron form-factors was made quite recently.[7] The new theoretical value is in good agreement with experiment

$$\begin{aligned} &\delta_{exp}(n=2) = 1057.86 \pm 0.06 \ MHz \\ &\text{old: } \delta_{th}(n=2) = 1057.56 \pm 0.08 \ MHz \\ &\text{new: } \delta_{th}(n=2) = 1057.91 \pm 0.16 \ MHz \end{aligned} \qquad (2.22)$$

The measurements of the static e.m. moments of $e^{\pm}$ and $\mu^{\pm}$ is of great interest not only as a check on QED, but also for the reasons of tests of the discrete symmetries P, C and T. For example, the experimental equality of the g-factors of electron and positron (within I ppm) and of muon and antimuon (at the level of 0,7 ppm), permits us to rule out any violation of TCP in the lepton g-factors at the level of I ppm.[8] From here on, we shall assume, that the theory is P-, C- and T- invariant. The matrix element of the e.m. current j_μ, sandwiched by the spinor particle states is

$$\langle p_2 | j_\mu(0) | p_1 \rangle = (2\pi)^{-3} \sqrt{\frac{m^2}{\varepsilon_2 \varepsilon_1}} \bar{u}(p_2) \left[\gamma_\mu F_1(q^2) + i \sigma_{\mu\nu} F_2(q^2) \right] u(p_1) \ , \quad q = p_2 - p_1 \qquad (2.23)$$

The Dirac (F_1) and Pauli (F_2) form factors give the "normal" (i.e. the Dirac) and anomalous magnetic moment distribution and satisfy the normalization

$$F_I(0) = e$$
$$\mu = \frac{F_1(0)}{2m} + F_2(0) \qquad (2.24)$$

Our initial Lagrangian has no dimensional coupling constant, as we have introduced the lepton-photon interaction in a "minimal" way i.e. using the gauge-invariant substitution (2.5). This means, that $F_2(0)$ should be found in terms of the charge and mass of the lepton in question:

$$F_2(0) = \frac{e}{2m} \sum_{n=1}^{\infty} A_n \left(\frac{\alpha}{\pi}\right)^n \qquad (2.25)$$

where A_n are the dimensionless numbers.

In table 3 comparison is given of the theoretical values of A_n's with experiment[9].

Table 3

Comparison between the theory and experiment for the lepton anomalous magnetic moments

		A_1	A_2	A_3
e^-	exp	0,5	-0,3285	$-7 \pm 2,4$
	th	-"-	-"-	$0,I3 \div 0,5$
μ^-	exp	-"-	+0,76578	49 ± 25
	th	-"-	-"-	23 ± 3

We have represented the experimental results for $F_2(0)$ in the form of the expansion of Eq.(2.24)assuming the theoretical values for the coefficients A_1 and A_2. The calculations show us, that the role of the high energy region in the intergration over virtual momenta in the Feynman expression for the magnetic moment (Fig. 2a) as well as the sensitivity of the theoretical result to possible modification of QED at

small distances is quite different for electrons and muons. We shall illustrate it taking as an example the calculation of the Schwinger correction $A_1 = \frac{1}{2}$. Let us apply the dispersion technique and write the dispersion relation for the $F_2(t)$ ($t = q^2$):

$$F_2(t) = \frac{1}{\pi} \int_{4m^2}^{\infty} \frac{dt' \, Im F_2(t')}{t' - t} \qquad (2.26)$$

where m is the mass of a lepton.

In the lowest order of perturbation theory $ImF_2(t)$, corresponding to the Feynman diagram of Fig. 2 (a), is of the form

$$Im F_2(t) = \frac{e}{2m} \frac{\alpha m^2}{\sqrt{t(t-4m^2)}} \qquad (2.27)$$

The explicit calculation of $F_2(0)$, using Eqs.(2.26) and (2.27) shows, that 99% of the exact value of $A_1 = \frac{1}{2}$ is coming from the integration of Eq.(2.26) over the region $4m^2 \leq t \leq 200m^2$. In the case of the electron the upper bound amounts to $t_{max} = 200\ m_e^2 = 50\ MeV^2$, while for the muon we have $t_{max} = 200\ m_\mu^2 = 2{,}15\ GeV^2$.

Thus, $F_2^\mu(0)$ should be much more sensitive to possible breaking of QED at small distances. Due to its small mass the free electron is a kind of the system, which is "dynamically" isolated from the interactions with other fields and the present discrepancy between $(A_3)_{exp}$ and $(A_3)_{th}$ (see Table 3) looks rather intriguing. New determinations of the electron moment anomaly are highly desirable. Further improvement of the accuracy in the muon (g-2) experiment will

enable us to understand more deeply the modification of "pure" QED by the weak and strong interactions and to search for both the specific μ-structure and the breaking of the fundamental principles of quantum field theory. We conclude with a note, that the photon propagator, modified according to Eq.(2.18), leads to the modification of a_{th} ($a = \frac{g-2}{2}$) of the form

$$-\frac{\delta a_\mu}{a_\mu} = \frac{2}{3}\frac{m_\mu^2}{\Lambda^2} \qquad (2.28)$$

Equating Eq.(2.28) to the experimental error for a^{μ}_{exp}, we get

$$\Lambda > 5 \text{ GeV} . \qquad (2.29)$$

It should be noted also, that all the tests of QED depend strongly on the precise value of the fine structure constant α :

$$\alpha^{-1} = 137,03608 \pm 0,00026 \ (1,9 \text{ ppm}) \qquad (2.30)$$

which was obtained by using the ratio $2\frac{e}{h}$, determined via the Josephson effect in superconductors.[6]

The theoretical calculations of the high order Feynman graphs become manageable since the development of powerful computer methods. The sixth order diagram of Fig. 2 (c) (the photon-photon scattering contribution) is found to be important for the evaluation of the muon moment anomaly

$$(\Delta a_\mu)_{\gamma-\gamma} = (18,4 \pm 1,1)\frac{\alpha^3}{\pi^3} \qquad (2.31)$$

and it was obtained numerically.[9]

To summarize, we can only repeat that the quantum electrodynamics seems to work as well as the initials imply (QED

= Quod Erat Demonstrandum).

3. LOW ENERGY THEOREMS, DISPERSION RELATIONS AND SUM RULES.

3.I General properties of the hadron e.m. current

There is no field theory of the hadron interaction at our disposal. So, the field equation

$$\Box A_\mu(x) = -\mathcal{J}_\mu^{e.m}(x)$$
$$\partial_\mu A^\mu(x) = 0 \qquad (3.I)$$

is just the definition of the hadron e.m. current J_μ .

As in the case of the lepton electrodynamics, we shall assume the validity of the current conservation

$$\partial_\mu J^\mu(x) = 0 \qquad (3.2)$$

and the gauge invariance conditions

$$K_\mu M_{\mu\nu\ldots} = q_\nu M_{\mu\nu\ldots}(p_1,\ldots,q,\ldots)=0 \qquad (3.3)$$

where $M_{\mu\nu..}$ is the hadronic part of arbitrary matrix element including the real or virtual photons. (Note, that Eq.(3.3) follows from Eq.(3.2) only for the one-photon amplitudes). We state now the properties of J_μ under the internal symmetry transformations. The eigenvalues of the electric charge operator

$$\hat{Q} = \int d^3x\, J_0(x) \qquad (3.4)$$

obey the Gell-Mann-Nishijima relation

$$Q = I_3 + \tfrac{1}{2} Y \qquad (3.5)$$

where I_3 and Y is the third component of the isospin and hypercharge, respectively. The local form of Eq.(3.5)

$$J_\mu = e\,(J_\mu^{V_3} + J_\mu^{S}) \equiv e\,(J_\mu^{3} + \frac{1}{\sqrt{3}} J_\mu^{8}) \qquad (3.6)$$

is assumed to be valid as well.

In Eq.(3.6) $J_\mu^{V_3\,(S)}$ is the isovector (isoscalar) part of the e.m. current, i = I, 2,... 8 are the SU(3) indices. Writing Eq.(3.6), we have fixed the tensor properties of $J_\mu^{e.m}$ both in the isospin and unitary space, as well as the transformation properties under the (generalized) charge conjugation

$$G J_\mu^{S(V_3)} G^{-1} = \mp J_\mu^{S(V_3)} \qquad (3.7)$$

$$C J_\mu C^{-1} = - J_\mu$$

$$G = C \cdot \exp(- i\pi \hat{I}_2) \qquad (3.8)$$

where C (G) is the (generalized) charge cojugation operator, $\hat{I}_i$ is the i-th component of the isospin.

3.2 The emission and absorption of soft γ-quanta.

We start our discussion of the dynamics of the e.m. interaction of hadrons with the consideration of the low energy theorems (LET) and dispersion sum rules i.e. the questions which are least dependent on particular dynamical models.

LET results in the exact limiting expression for the amplitudes of absorption and emission of the zero energy γ-quanta.

Let

$$T(A \rightleftarrows B + \gamma) = \epsilon_\mu T_\mu(p_1, \ldots p_n ; k) \qquad (3.9)$$

be the amplitude of an arbitrary photon process $A \rightleftarrows B + \gamma$ with all particles lying on their mass shells $p_i^2 = m_i^2$,

$k^2 = 0$. The theorem states, that the coefficients c_{-1} and c_0 in the expansion

$$\lim_{K\to 0} T(A \rightleftharpoons B+\gamma) = \sum_{n=-1}^{\infty} c_n K^n = \frac{c_{-1}}{K} + c_0 K^0 + O(K) \qquad (3.10)$$

are defined in terms of the static e.m. properties of the particles involved (charge, magnetic moment etc.) and the radiationless amplitude $T(A \rightleftharpoons B)$.

As an example we list several processes in Table 4, pointing out which characteristics of the reaction $A \rightleftharpoons B$ are needed to describe the amplitude $T(A \rightleftharpoons B+\gamma)$ at $k \to 0$.

T a b l e 4

Dynamical quantities needed for description of radiative processes at low photon energies.

	Reaction $A \rightleftharpoons B + \gamma$	$A \rightleftharpoons B$	$T(A \rightleftharpoons B)$
I.	$N + N \to N + N + \gamma$	$N + N \to N + N$	phase-shifts of NN-scattering
2.	$\gamma + N \to \gamma + N$	$N \to N + \gamma$	e.m. form factors of nucleons
3.	$\gamma + N \to \pi + N$	$N \to N + \pi$	$g_{\pi NN}$ coupling constant
4.	$\gamma + D \to n + p$	$D \to p + n$	g_{Dpn} coupling constant, or deuteron wave function

Due to the zero photon mass only the processes of the photon emission and scattering are thresholdless. In this case Eq.(3.10) defines the amplitude in the physical region of a given process. The reactions of the pion production and

nuclear photodisintegration are the threshold ones and the value $k = 0$ is in non-physical region. Special consideration is needed to decide whether Eq.(3.I0) can be used at $\omega \geq \omega_{thr.} > 0$ and to compute the corrections, if necessary.

There are several equivalent methods to prove LET. We explain the general idea using the Low's approach[I0]. The proof is based on the masslessness of photon, the gauge condition (3.3) and the lowest order approximation in α.

The amplitude (3.9) gets contributions from two types of terms

$$T_\mu = T_\mu^{ext} + T_\mu^{int} \qquad (3.II)$$

where $T^{ext(int)}$ represent the Feynman diagrams in which the photon line is ended on the external (internal) particle lines. Owing to the zero mass of photon, T_μ^{ext} has the singularity at the point $k=0$:

$$T_\mu^{ext}(K) = \sum_i \frac{N_\mu^i(K)}{(p_i \pm K)^2 - m_i^2} \equiv \frac{C_{-1}}{K} + \tilde{C}_0 + O(K) \qquad (3.I2)$$

There are no internal virtual photon lines in the diagrams we consider, since we confined ourselves only to lowest order approximation in α. Therefore, we have

$$T^{int} = T^{int}(0) + O(k) \qquad (3.I3)$$

where $T^{int}(0)$ is regular at $k = 0$.

Define now new amplitudes

$$T_\mu^I = \frac{C_{-1}}{K} + \tilde{C}_0 K^0 + C_R + O(K) \equiv \frac{C_{-1}}{K} + C_0 + O(k) \qquad (3.I4)$$

$$T_\mu^{II} = T_\mu^{int}(0) - C_R \qquad (3.I5)$$

where we have introduced the constant C_R, which should be defined from the condition

$$k_\mu T^I_\mu = 0\,(k^2) \quad . \tag{3.16}$$

The gauge condition (3.3) imposes

$$K_\mu (T^I_\mu + T^{II}_\mu) = 0 \quad . \tag{3.17}$$

Taking into account Eq.(3.16), we get finally

$$\begin{aligned} T_\mu &= T^I_\mu + O(K) \quad , \\ T^{II}_\mu &= O(K) \quad , \end{aligned} \tag{3.18}$$

which proves the statement (3.10), because T^I_μ is expressed in terms of the e.m. properties of "external" particles and the characteristics of the process T ($A \rightleftarrows B$). As an example, we consider below the Compton scattering on nucleon and make use of LET to be derived, to obtain the dispersion sum rules for the photoabsorption cross sections.

3.3 Divergence condition and low energy theorems for the "isovector" Compton scattering.

The e.m. currents, entering the Compton scattering amplitude, include, according to Eq.(3.6), both the isoscalar and isovector parts. For the sake of generality and to emphasize some important points we consider the matrix elements of the conserved isoscalar (J^S_μ) and isovector (J^a_μ, a=1,2,3) currents separately. These matrix elements will be referred to the "isoscalar" and "isovector" photon scattering on nucleons

$$T^{ss}_{\mu\nu} = T(\gamma^S N \to \gamma^S N) \tag{3.19}$$

$$T_{\mu\nu}^{\alpha\beta} = T(\gamma^{\alpha} N \to \gamma^{\beta} N) \; ; \quad \alpha, \beta = 1,2,3. \tag{3.20}$$

The isotopic structure of the amplitude (3.20) is similar to that of the π -N scattering amplitude

$$T_{\mu\nu}^{\alpha\beta} = \delta_{\alpha\beta} T_{\mu\nu}^{(+)} + \frac{1}{2} [\tau_{\alpha}, \tau_{\beta}] T_{\mu\nu}^{(-)} \tag{3.21}$$

The fact of the extreme importance is that the gauge condition (3.3) is replaced now by the non-zero divergence condition

$$K_{\mu} M_{\mu\nu}^{\alpha\beta} = i \epsilon_{\alpha\beta c} V_{\nu}^{c} \equiv V_{\nu}^{[\alpha,\beta]} \neq 0 \tag{3.22}$$

What is $V_{\nu}^{[\alpha,\beta]}$ in Eq.(3.22) equal to?

One can obtain the exact and model - independent limiting expression for V_{ν} at $k_1 \to 0$ or / and $k_2 \to 0$. According to preceding consideration it is given by the pole diagrams, represented in Fig.3.

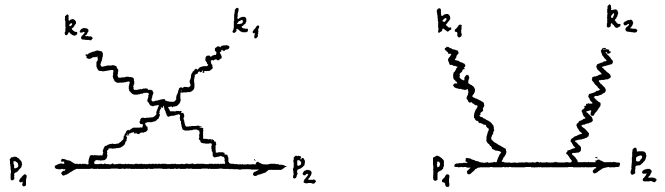

Fig. 3 Pole diagrams for the Compton scattering.

Direct calculation gives

$$\lim_{K_1 \to 0} K_{1\mu} T_{\mu\nu}^{\alpha\beta} = [\tau_{\beta}, \tau_{\alpha}] \bar{u}(p_2) \Big[F_1^{v}(0) \gamma_{\nu} + \frac{F_2^{v}(0)}{2m} \frac{\gamma_{\nu} \hat{K}_2 - \hat{K}_2 \gamma_{\nu}}{2} \Big] u(p_1) \tag{3.23}$$

$$\lim_{K_2 \to 0} T_{\mu\nu}^{\alpha\beta} K_{2\nu} = [\tau_{\beta}, \tau_{\alpha}] \bar{u}(p_2) \Big[F_1^{v}(0) \gamma_{\mu} - \frac{F_2(0)}{2m} \frac{\gamma_{\mu} \hat{K}_1 - \hat{K}_1 \gamma_{\mu}}{2} \Big] u(p_1) \tag{3.24}$$

The current algebra approach gives us the model - dependent result for arbitrary values of k_1 and k_2

$$K_{1\mu} T^{\alpha\beta}_{\mu\nu} = 2i \epsilon_{\alpha\beta c} \tau_c \bar{u}(p_2) \left[F_1^V(q^2) \gamma_\nu + \right.$$
$$\left. + i \frac{F_2^V(q^2)}{2m} \sigma_{\mu\nu} q_\nu \right] u(p_1) , \quad q = K_1 - K_2 = p_2 - p_1 \tag{3.25}$$

which is consistent with Eq.(3.23) at $k_1 \to 0$.

The vector current conservation

$$\partial_\mu J^\alpha_\mu(x) = 0$$

implies the vanishing of the divergence of one - current (or, equivalently, one - "isovector - photon") amplitudes as well as the imaginary parts of the two - current ("Compton") amplitudes:

$$K_\mu T^\alpha_\mu = i K_\mu \int d^4x\, e^{iKx} \langle n | T^\alpha_\mu | p \rangle = - \int d^4x\, e^{iKx} \langle n | \partial_\mu J^\alpha_\mu | p \rangle = 0 \tag{3.26}$$

$$K_{1\mu}\, Im\, T^{\alpha\beta}_{\mu\nu} = Im\, T^{\alpha\beta}_{\mu\nu} K_{2\nu} \propto K_{1\mu} \sum_n \langle p_2 | J^\beta_\nu | n \rangle \langle n | J^\alpha_\mu | p_1 \rangle = 0 \tag{3.27}$$

The non-zero divergence condition (3.25) leads to important consequences. Firstly, it follows from Eqs.(3.25) and (3.27) that the real part of $T_{\mu\nu}$ has the non - Regge fixed (i.e. independent of the momentum transfer) power polynomial behaviour in energy. Secondly, we should now use Eq.(3.25) instead of Eq.(3.3) in derivation of LET for $T^{ab}_{\mu\nu}$ and define the constant C_R in Eqs.(3.I4) and (3.I5) from

$$K_{1\mu}\, T^{\alpha\beta\,(I)}_{\mu\nu} = V^{[\alpha,\beta]}_\nu + O(\omega^2),$$
$$K_{2\nu}\, T^{\alpha\beta\, I}_{\mu\nu} = V^{[\alpha,\beta]}_\mu + O(\omega^2). \tag{3.28}$$

We write down the explicit formulae for the forward scattering ($k_1 = k_2 = k$) amplitude only.

$$T_{\mu\nu}^{\{\alpha\beta\}}(Born) = \frac{1}{2}\{\tau_\alpha, \tau_\beta\}\bar{u}(p)\Big[-\frac{F_1^v(0)^2}{2(p\cdot k)}\cdot 2g_{\mu\nu}\hat{k} + \\ + \Big(\frac{F_2^v(0)}{2m}\Big)^2 \times (\gamma_\mu\gamma_\nu - \gamma_\nu\gamma_\mu)\hat{k}\Big]u(p), \qquad (3.29)$$

$$T_{\mu\nu}^{[\alpha,\beta]}(Born) = \frac{1}{2}[\tau_\alpha, \tau_\beta]\bar{u}(p)\Big[-\frac{F_1^v(0)^2}{2(p\cdot k)}(\gamma_\mu\gamma_\nu - \gamma_\nu\gamma_\mu)\hat{k} + \\ + \Big(\frac{F_2^v(0)}{2m}\Big)^2\cdot 2g_{\mu\nu}\hat{k}\Big]u(p), \qquad \hat{k} = \gamma_\mu k^\mu, \qquad (3.30)$$

$$g_{oo} = -g_{11} = -g_{22} = -g_{33} = 1\ ;\ g_{\mu\nu} = 0,\ \mu \neq \nu,$$

where $\{\ldots\}$ denotes the anticommutator of the Pauli isospin matrices τ_i, while $[\ldots]$ stands for the commutator.

Corresponding superscripts in T's define the symmetric part and antisymmetric one in the isospin indices.

Symmetrical amplitude (3.29) and, in particular, the "physical" Compton scattering amplitudes, satisfy the zero divergence conditions, as they should do. Hence,

$$T_{\mu\nu}^{\{\alpha,\beta\}I} = T_{\mu\nu}^{\{\alpha,\beta\}}(\text{Born}) \qquad (3.31)$$

In the antisymmetrical case an additional term is required

$$T_{\mu\nu}^{[\alpha,\beta]I} = T_{\mu\nu}^{[\alpha,\beta]}(\text{Born}) + T_{\mu\nu}^{[\alpha,\beta]'} \qquad (3.32)$$

From Eq.(3.28) $T_{\mu\nu}^{[\alpha,\beta]'}$ is found to be

$$T_{\mu\nu}^{[\alpha,\beta]'} = \frac{1}{2}[\tau_\alpha, \tau_\beta]\bar{u}(p)F_1^v(0)\Big[4F_1^v(0)'g_{\mu\nu} - \frac{F_2(0)}{2m}(\gamma_\mu\gamma_\nu - \gamma_\nu\gamma_\mu)\Big]u(p) \qquad (3.33)$$

With the help of Eqs.(3.29) – (3.33) we can find the low-energy behaviour each of T's in general form of the forward Compton scattering amplitude

$$T_{ij}^{\alpha\beta}(\omega) = \delta_{\alpha\beta}\left(T^{++}\delta_{ij} + i\epsilon_{ijk}\sigma_k T^{+-}(\omega)\right) + \\ + \frac{1}{2}[\tau_\alpha, \tau_\beta]\left(\delta_{ij}T^{-+}(\omega) + i\epsilon_{ijk}\sigma_k T^{--}(\omega)\right), \qquad (3.34)$$

where indices i, j = I, 2, 3 are understood to be contracted with the polarization 3-vectors of photons.

3.4 Dispersion relations and FESR.

It follows from the causality and spectrality (i.e. completeness of the positive energy state - vectors) that $T_{ij}^{\alpha\beta}$ is an analytical function of z ($Re\, z = \omega$) in the region of complex plane, limited by contour C_R , as shown in Fig. 4. Therefore we can apply the Cauchy formula

$$T(z) = \frac{1}{2\pi i} \oint_{C_R} \frac{T(z')}{z'-z}\, dz' \qquad (3.35)$$

to define

$$T^{\pm\pm}(0) = \frac{1}{2\pi i} \oint_{C_R} \frac{T^{\pm\pm}(z)}{z}\, dz \qquad (3.36)$$

$$T^{\pm\mp\,\prime}(0) = \frac{1}{2\pi i} \oint_{C_R} \frac{T^{\pm\mp}(z)}{z^2}\, dz \qquad (3.37)$$

To derive the sum rules for each of four functions in Eq. (3.34), we have

a) to substitute the left - hand sides in Eqs.(3.36) and (3.37) for their zero-energy limits found from Eqs.(3.29) - (3.32).

b) to exclude the integrals over $-R \leq \omega \leq 0$, using the crossing-symmetry relations

$$T^{\pm\pm}(\omega) = +T^{\pm\pm\,*}(-\omega)$$
$$T^{\pm\mp}(\omega) = -T^{\pm\mp\,*}(-\omega) \qquad (3.38)$$

c) to express the integrals over $0 \leq \omega \leq +R$ through the optical theorem

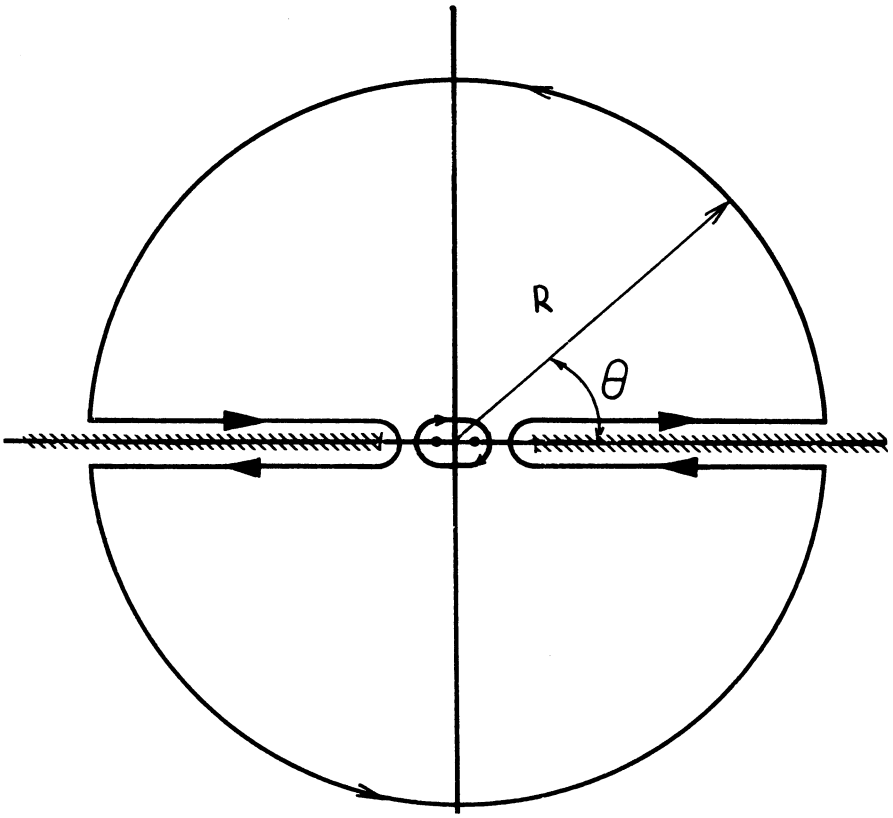

Fig. 4 The contour of integration in the Cauchy formula.

$$Im\,T^{++}(\omega)=\frac{\omega}{4\pi}\;\frac{\sigma_p^{+}+\sigma_a^{+}}{2} \tag{3.39}$$

$$Im\,T^{-+}(\omega)=\frac{\omega}{4\pi}\;\frac{\sigma_p^{-}+\sigma_a^{-}}{2} \tag{3.40}$$

where

$$\sigma^{\pm}=\frac{1}{2}\left[\sigma^{(+)}\pm\sigma^{(-)}\right]\equiv\frac{1}{2}\left[\sigma(\gamma^{+}N)\pm\sigma(\gamma^{-}N)\right],$$

$\sigma_{p(a)}$- the cross section of photon-nucleon interaction when spin of the photon polarized parallel (antiparallel) to that of nucleon.

We write down the final form of sum rules

$$-\frac{\alpha}{4m}=\frac{1}{2\pi^2}\int_{\omega_0}^{R}\sigma^{v}(\omega)d\omega+C_R^{++}, \tag{3.4I}$$

$$\alpha\frac{(\varkappa_p-\varkappa_N)^2}{8m^2}=\frac{1}{4\pi^2}\int_{\omega_0}^{R}\frac{d\omega}{\omega}(\sigma_p^{v}-\sigma_a^{v})+C_R^{+-}, \tag{3.42}$$

$$\alpha\left[\frac{(\varkappa_p-\varkappa_n)^2}{8m^2}-\frac{1}{6}\left(\langle r_1^2\rangle_p-\langle r_1^2\rangle_n\right)\right]=\frac{1}{4\pi^2}\int_{\omega_c}^{R}\frac{d\omega}{\omega}(\sigma^{(+)}-\sigma^{(-)})+C_R^{-+}, \tag{3.43}$$

$$-\alpha\frac{\mu_p-\mu_n}{4m}=\frac{1}{8\pi^2}\int_{\omega_0}^{R}d\omega\,(\sigma_p^{(+)}-\sigma_a^{(+)}-\sigma_p^{(-)}+\sigma_a^{(-)})+C_R^{--}, \tag{3.44}$$

where C_R stands for the integral over the circle of radius R in Fig. 4, and the indices attached to C_R show which of four functions in Eq.(3.34) the whole sum rule should be referred to.[11)]

Writing Eqs.(3.4I) - (3.44) we have used the notations

$$\sigma^{v}\equiv\frac{1}{2}\left(\sigma^{(+)}+\sigma^{(-)}\right) \tag{3.45}$$

$$F_{1,2}^{V} = \frac{1}{2}\left(F_{1,2}^{p} - F_{1,2}^{n}\right) \tag{3.46}$$

$$F_1'(0) = -\frac{1}{6}\langle r_1^2\rangle, \quad F_2(0) = \varkappa, \tag{3.47}$$
$$\mu = F_1(0) + F_2(0)$$

and P (n) denotes a proton (neutron).

The cross sections entering sum rules (3.4I) - (3.44) cannot be measured directly in photon reactions but they can, in principle, be evaluated using the multipole (or phase-shift) analysis of the meson photoproduction amplitudes. Sum rules, analogous to Eq.(3.4I) and (3.42), can be proposed for the measurable "real" photon-nucleon cross sections

$$-\frac{\alpha}{m} = \frac{1}{2\pi^2}\int_{\omega_0}^{R} \sigma_{tot}^{\gamma p}(\omega)\,d\omega + C_R^{p+} \tag{3.48}$$

$$\frac{\alpha \varkappa_p^2}{2m^2} = \frac{1}{4\pi^2}\int_{\omega_0}^{R} \frac{d\omega}{\omega}\left(\sigma_p^{\gamma p}(\omega) - \sigma_a^{\gamma p}(\omega)\right) + C_R^{p-} \tag{3.49}$$

with an evident modification in the case of the neutron target.

The finite energy ($R < \infty$) sum rules (3.4I) - (3.44) and (3.48), (3.49) are valid for any value of R. Let us consider now the case of large R , when the Compton amplitude has, presumably, the asymptotic expansion of the form:[12]

$$T(\omega, t) \xrightarrow[\omega\to\infty]{} -\sum_{\tau} G_\tau(t)\,\frac{\tau_\tau + e^{-i\pi\alpha_\tau(t)}}{\sin\pi\alpha_\tau(t)}\,\omega^{\alpha_\tau(t)} + \tag{3.50}$$
$$+\sum_{\kappa=1}^{\infty} f_\kappa(t)\left(\frac{1}{\omega}\right)^{\kappa}\left(1+\eta(-1)^{\kappa}\right)$$

The first term in Eq.(3.50) represents the ordinary Regge -

pole contribution and the second one is non-Regge term, which in the language of the complex J-plane approach is related to the fixed poles. In Eq.(3.50) η is the crossing phase ($\eta = +I$ for $T^{\pm\pm}$, $\eta = -I$ for $T^{\pm\mp}$), τ, $G_\tau(t)$ and $\alpha(t)$ are the signature, residue and trajectory of the Regge-pole, respectively. One can obtain now

$$C_R^e = -\frac{2}{\pi}\sum_\tau G_\tau^e(0)\frac{R^\alpha}{\alpha} + 2f_0(0) , \qquad (3.5I)$$

$$C_R^o = -\frac{2}{\pi}\sum_\tau G_\tau^o(0)\frac{R^{\alpha-1}}{\alpha-1} + 2f_{-1}(0) , \qquad (3.52)$$

where $C_R^{e(0)}$ is related to the crossing - even (odd) amplitudes $T^{\pm\pm}(T^{\pm\mp})$.

Quantum numbers of the leading Regge - trajectories are listed in Table 5.

T a b l e 5

Quantum numbers of leading Regge - trajectories

Amplitude	τ	P	I	G	Symbol
T^{++}	+I	+	0	+	P,P' - vacuum Pomeranchuk poles.
T^{+-}	-I	+	0	+	$J^P = I^+$-mesons: D(?),...
T^{-+}	-I	-	I	+	ρ
T^{--}	+I	-	I	+	?

As $\alpha_\rho(0) = I$, the sum rules (3.4I) and (3.48) are meaningful only for $R < \infty$. The other sum rules may happen

to be "superconvergent" ones i.e. they might be finite even at $R \to \infty$.

Unknown constants f_0 and f_{-1} contribute only to the real parts of the corresponding amplitudes. For energy dependence of these fixed pole contributions is similar to that given by the Born diagrams (Fig.3), one can, conventionally, to speak of them as of the part of the Born terms, which "survive" at high energies.

3.5 Consequences on the total photoabsorption cross sections from sum rules.

What are the results we get from the comparison of sum rules with experimental data?

3.5.I. Energy dependence.

The measurements of the total cross section $\sigma_{\gamma p}(\omega)$ in high energy region (say, $\omega \geq 3$ GeV) can be used to determine the parameters of "effective" vacuum pole

$$\sum_{\tau=\rho,\rho'} G_\tau \omega^{\alpha_\tau} = G_{eff}\, \omega^{\alpha_{eff}} \qquad (3.53)$$

with the help of sum rules

$$\int_{R_1}^{R_2} \omega^n \sigma_{tot}^{\gamma p}(\omega)\, d\omega = \frac{1}{2\pi^2} \frac{G_{eff}}{\alpha_{eff}+n} \left(R_2^{\alpha_{eff}+n} - R_1^{\alpha_{eff}+n}\right) \qquad (3.54)$$

$$n = 0, 2.$$

For given $R_1 \leq \omega \leq R_2$, the values of α_{eff} are very close for the pion-nucleon and photon-nucleon interactions. This fact means, that

$$\frac{G_\rho(\pi)}{G_\rho(\gamma)} \simeq \frac{G_{\rho'}(\pi)}{G_{\rho'}(\gamma)} \simeq \frac{\sigma(\pi^+ p)+\sigma(\pi^- p)}{\sigma(\gamma p)} \simeq const \qquad (3.55)$$

Fig. 5 demonstrates the similarity of the energy dependence of the pion-nucleon and photon-nucleon cross section at high energy.[13]

3.5.2. Isospin dependence.

We continue the line of comparison of π N- and γ N- cross sections. We note, that the Cabibbo-Radicati sum rule (which is nothing, but Eq.(3.43) with $R\to\infty$ and $C^{-+}\to 0$)

$$2\pi^2\left(\frac{e^2}{4\pi}\right)\frac{1}{m^2}\left[\frac{(\varkappa_p-\varkappa_n)^2}{4}-\frac{m^2}{3}\left(\langle r_1^2\rangle_p-\langle r_1^2\rangle_n\right)\right]=\int_{th}^{\infty}\frac{d\omega}{\omega}\left(\sigma_\gamma^{(+)}-\sigma_\gamma^{(-)}\right) \tag{3.56}$$

has the structure similar to the famous Adler-Weissberger sum rule for the axial-vector coupling - constant renormalization in β -decay

$$2\pi^2\left(\frac{g^2_{\pi NN}}{4\pi}\right)\frac{1}{m^2}\left(1-\frac{1}{g_A^2}\right)=\int_{th}^{\infty}\frac{d\omega}{\omega}\left(\sigma_\pi^{(+)}-\sigma_\pi^{(-)}\right), \tag{3.57}$$

where $g^2_{\pi NN}/4\pi = 14{,}6$ and $g_A = -1{,}23$.

We point now to one qualitative feature of the isospin dependence of nucleon excitation by pions and "isovector" photons. In Eq.(3.56) the Born-term contribution (e.g. the first term in the left-hand side of Eq.(3.56)) is less than the current-algebra contribution (the second term in the left-hand side of (3.56)), while in Eq.(3.57) just vice versa: the current-algebra contribution is less than that of the Born term. Thus, in total, the left-hand side of Eq.(3.56) is negative, while in Eq.(3.57) it is positive.

Taking into account, that

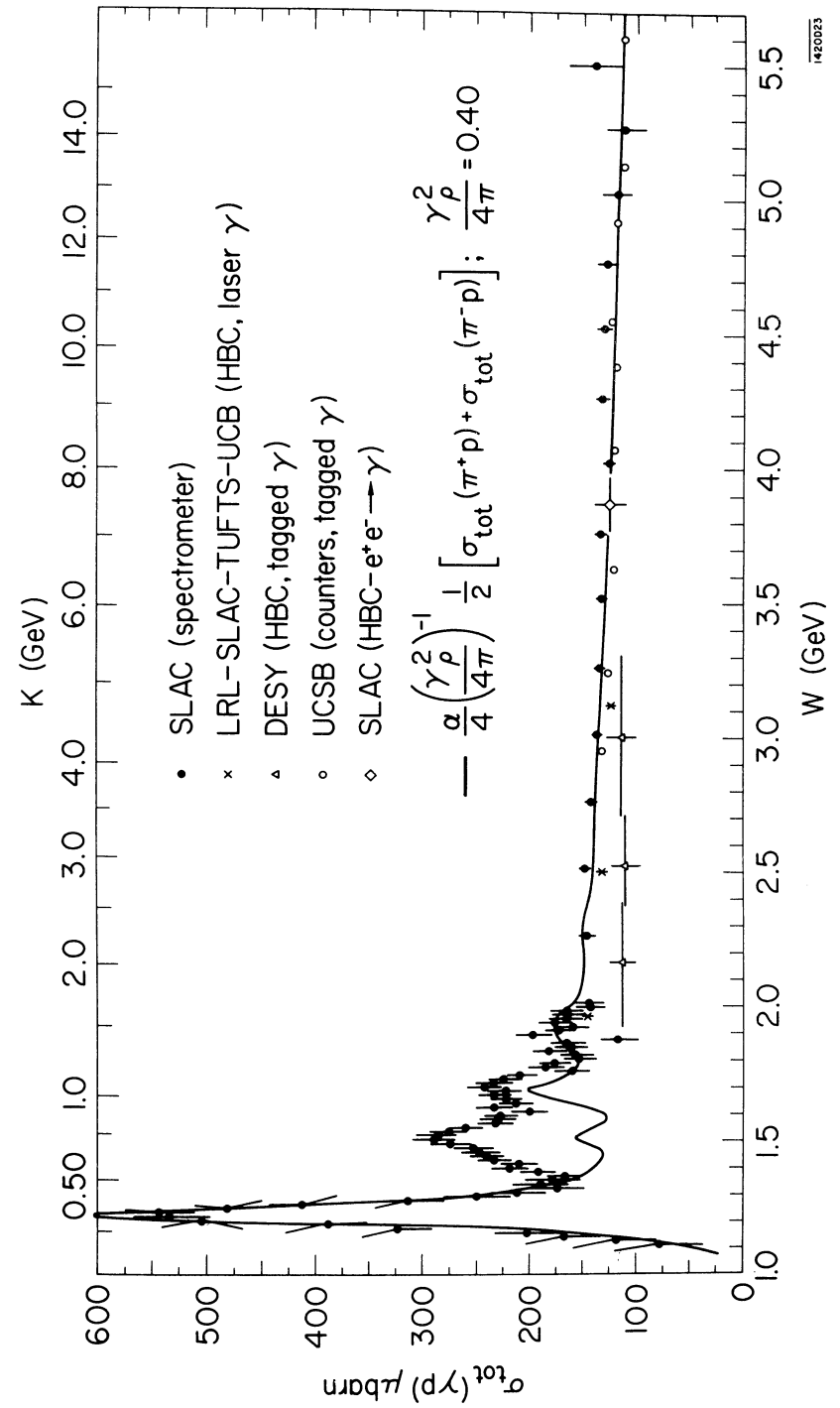

Fig. 5 Comparison of the energy dependence of the total photon-nucleon and pion-nucleon cross-sections. (From Ref. 13).

$$\sigma^{(+)} - \sigma^{(-)} = \frac{2}{3}\left(\sigma(I=3/2) - \sigma(I=1/2)\right) \qquad (3.58)$$

we conclude, that the excitation of the $I = 1/2$ final states, in comparison with the $I = 3/2$ - states, goes much stronger in photon reactions than in the pion induced reactions. This is especially clearly seen in the region of nucleon resonances with masses around I,5 - I,6 GeV (see Fig. 5). From this conclusion it follows also, that in the pion photoproduction and Compton scattering in backward direction, where the u-channel baryon exchanges are commonly assumed to be dominating, in addition to the nucleon (N_α) and Δ(I236) - trajectories one should include at least one more Regge-trajectory with $I = 1/2$ (the so - called N_γ - trajectory, which goes through the first two resonances N^*, which are $N^*(1520, J^P = 3/2^-)$ and $N^*(2190, J^P = 7/2^-)$).

3.5.3. Spin dependence.

Due to the lack of direct experimental measurements of σ_ρ and σ_a, entering the anomalous magnetic moment sum rules (3.42) and (3.49), one must construct them from multipole analyses of pion photoproduction. The calculations available[12] appear to confirm the validity of these sum rules, together with basic underlying assumption on the spin independence of cross sections at high energies. Numerically, it was found,[14] that the only contribution of Δ -resonance gives good "saturation" of these sum rules (with an accuracy of about I0 - I5%). To compensate the negative contribution to the

sum rules from the nonresonant s-wave of π N photoproduction (evidently, it contributes only to σ_a, because of angular momentum conservation) the higher resonances N^* (I520, $J^P = 3/2^-$) and N^*(I688, $J^P = 5/2^+$) should contribute mainly to σ_p. This is just the case,[15] as is seen from forward and backward pion photoproduction.

The corresponding differential cross sections do not show any resonant peaks at the place of "second" and "third" π N-resonances, while the total cross sections do. Hence, these resonances are excited mainly in the state with parallel spins of photon and nucleon. Angular momentum conservation forbid them to contribute to forward and backward pion photoproduction in that case.

3.5.4. Possible evidence for fixed poles.

The interesting evidence for the fixed pole in $T^{p+}(\omega)$ was discovered recently from the analysis of the dispersion sum rules[16] and dispersion relations for the forward γp -scattering.[17] The value of the fixed pole contribution in $Re\,T^{p+}(\omega)$ at $\omega \to \infty$ was found to be of the order of the Thomson value

$$Re\,T^{p+}(0) = -\frac{\alpha}{m} \qquad (3.59)$$

The fixed poles may happen to be inherent only to "weak" amplitudes and be absent in the pure hadron amplitudes. Hence, in view of Eq.(3.55) and smallness of (3.59) the belief to get reasonable description of the high energy e.m. phenomena in terms of ordinary hadron-like phenomenology looks promising.

4. VECTOR MESON DOMINANCE MODEL AND MESON PHOTOPRODUCTION AT HIGH ENERGIES.

4.I Basic dynamical assumptions.

During the last two or three years great attention was paid to the vector meson dominance (VMD) model in the theory of hadron e.m. interaction.[18] In fact, VMD reduces the studies of the e.m. processes to the description of pure hadronic dynamics where vector mesons play the central role. Since the neutral vector mesons ρ^0, ω and φ have spin, parity and charge conjugation identical with the photon, they can decay into the lepton pair with the virtal photon in the intermediate state (see Fig. 6(a))

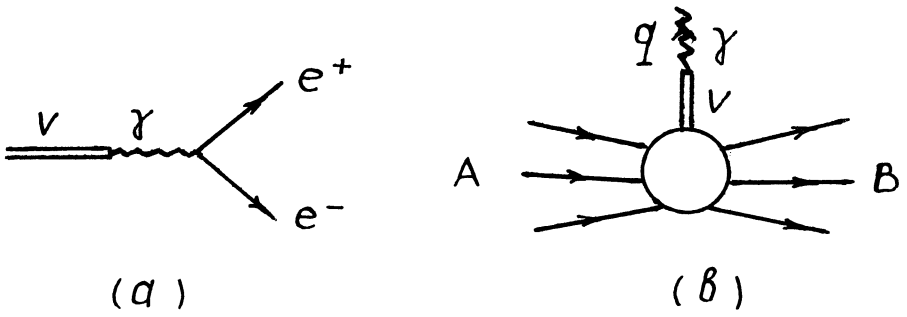

Fig. 6 Graphical representation of VMD.

Consider the matrix element of the e.m. current

$$T_\mu^\gamma = M_\mu^\gamma(p_A, p_B, q)\,\delta^{(4)}(p_A - p_B - q) = \langle B|\mathcal{J}_\mu^{e.m.}(0)|A\rangle\,\delta^{(4)}(p_A - p_B - q) \quad (4.I)$$

describing the process $A \rightleftarrows B + \gamma$ (Fig. 6(b)), where A and B are arbitrary hadronic states.

When $q^2 \to m_V^2$ $(V = \rho^0, \omega, \varphi)$ the matrix element (4.I)

should exhibit the resonance pole behaviour, owing to the existence of V-mesons:

$$M_\mu^\gamma(q^2 \to m_V^2) = \frac{G_{\gamma V} M_\mu^V(q^2)}{m_V^2 - q^2} + R(q^2) \simeq \frac{g_{\gamma V} m_V^2}{m_V^2 - q^2} M_\mu^V(m_V^2) \qquad (4.2)$$

where $G_{\gamma V} \equiv m_V^2 g_{\gamma V}$ is the γ-V coupling constant, $M_\mu^V(q^2 = m_V^2)$ is the amplitude of $A \rightleftarrows B + V$ and $R(q^2)$ represents possible nonresonant background.

The basic dynamical hypothesis of VMD is that of the smooth behaviour of $M_\mu^V(q^2)$ as we go away from $q^2 = m_V^2$. This smoothness assumption leads to the approximate equalities

$$T_\mu(A \rightleftarrows B + \gamma)\big|_{q^2=0} \simeq \sum_V g_{\gamma V} T_\mu(A \rightleftarrows B + V_{tr})\big|_{q^2=m_V^2} \qquad (4.3)$$

$$T_\mu(A \rightleftarrows B + \gamma(q^2 \neq 0)) \simeq \sum_V g_{\gamma V} \frac{m_V^2}{m_V^2 - q^2} T_\mu(A \rightleftarrows B + V)\big|_{q^2=m_V^2} \qquad (4.4)$$

which also can be obtained starting from the so-called current - field identity

$$J_\mu^{e.m.}(x) = \sum_{V=\rho^0,\omega,\varphi} g_{\gamma V} m_V^2 V_\mu(x) \qquad (4.5)$$

where $V_\mu(x)$ is the local field operator of V-meson ($V = \rho^0, \omega, \varphi$).

The important feature of Eq.(4.3) is the following. The polarization four-vector $\epsilon_\mu(q)$ has to obey the subsidiary Lorentz condition

$$q_\mu \epsilon^\mu = 0, \qquad (4.6)$$

to describe the unit-spin particle.

If $q^2 \neq 0$, then $\epsilon_\mu^\lambda(q)$ has three polarization states: two of them ($\vec{\epsilon}^{(\lambda=1,2)} \perp \vec{q}$) are transversely po-

larized, and the third one describes the longitudinally polarized state ($\vec{\epsilon}^{(\lambda=3)} \parallel \vec{q}$). On the other hand, if $q^2 = 0$ then $\epsilon_\mu^\lambda(q)$ has only two transversely polarized states. The essence of Eq.(4.3) is that the matrix element $T(A \rightleftarrows B + V_{tr})$, where V-meson is in the state with transverse polarization, does not vary much under extrapolation $q^2 \to 0$.

We shall consider below some applications of Eq.(4.3) to photoproduction of the pseudoscalar and vector mesons from nucleons and nuclei at high energies. The high-energy region is chosen for the following reasons.

The binary amplitudes

$$\gamma + A \rightleftarrows B + C \qquad (4.7a)$$

$$V + A \rightleftarrows B + C \qquad (4.7b)$$

satisfy certain crossing - symmetry relations under substitution $s \rightleftarrows u$. With fixed value of t, we have

$$u = -s - t + m_A^2 + m_B^2 + m_C^2 + \left\{ \begin{array}{l} 0 \quad \text{for Eq. (4.7a)} \\ m_V^2 \quad \text{for Eq. (4.7b)} \end{array} \right\} \qquad (4.8)$$

Clearly, Eq.(4.3) is approximately consistent with exact $u \rightleftarrows s$ crossing - symmetry and identity (4.8) only at $s \gg m_V^2$.

Further, the high-energy processes are dominated by small momentum transfers, typical dependence being

$$\frac{d\sigma}{dt} = A \exp(Bt), \quad B \simeq 5 \div 10 \ \text{GeV}^{-2} \qquad (4.9)$$

Hence, the distance between the physical t - region ($|t| \geq |t_{min}|$) and the nearest singularity in t - channel (which is either one pion exchange pole at $t = m_\pi^2$ or the

two-pion cut $t \geqslant 4\, m_\pi^2$) is of importance.

The numerical value of t_{min} depends on m_V^2. For instance,

$$t_{min}(\gamma N \to \rho N) \simeq -\left(\frac{m_\rho^2}{2\omega}\right)^2 \qquad (4.10a)$$

$$t_{min}(\gamma N \to \gamma N) = 0 \qquad (4.10b)$$

The difference between Eqs.(4.10a) and (4.10b) will disappear only when $\omega \to \infty$.

4.2 VMD and the vector meson photoproduction

According to Eq.(4.3) we have

$$T(\gamma N \to VN) = \sum_{V'} g_{\gamma V'}\, T(V'_{t_2} N \to VN) \qquad (4.11a)$$

$$T(\gamma N \to \gamma N) = \sum_{V',V''} g_{\gamma V'} g_{\gamma V''}\, T(V'_{t_2} N \to V''_{t_2} N)\,. \qquad (4.11b)$$

The differential cross sections for the elastic photon and vector meson scattering from nucleons have not been measured yet. There are experimental data on the neutral vector meson photoproduction and total photoabsorption on nucleons and nuclei, as well as some indirect data on $\sigma_{tot}(\rho^0 N)$ extracted from the coherent photoproduction of ρ^0's from complex nuclei.[19]

The energy dependence of $\sigma_{tot}(\gamma p \to Vp)$ is presented in Fig. 7. In the cases $V = \rho^0$ and φ the cross-sections vary smoothly, as in other processes of diffraction nature. Within experimental errors the energy dependence of $d\sigma(\gamma p \to \rho^0 p)$ is similar to that of the pion-nucleon elastic scattering. At $k \gtrsim 2.5$ GeV $\sigma(\gamma p \to \omega p)$

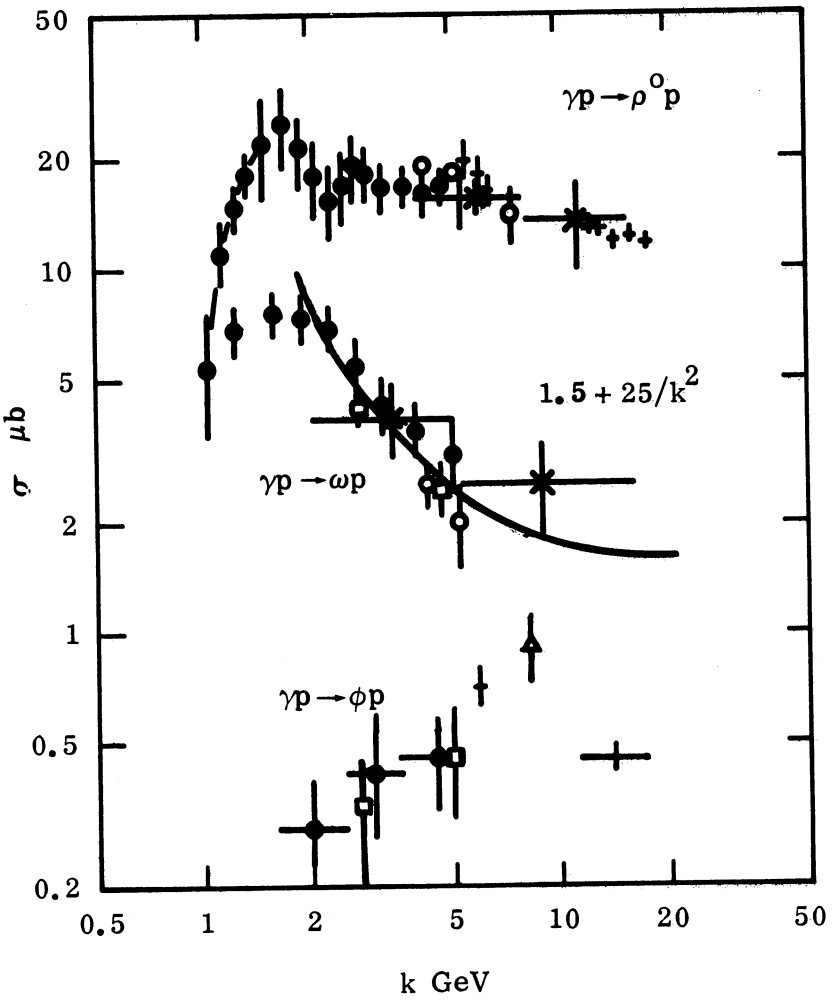

Fig. 7 Compilation of total cross-sections for vector meson photoproduction. (From Ref. 26).

fits rather well to the empirical formula

$$\sigma_{tot}(\gamma p \to \omega p) = \left(1{,}5 + \frac{25}{K^2}\right) \mu b \quad , \quad [K] = GeV \qquad (4.12)$$

The second term in Eq.(4.I2) displays the existence of non-diffractive mechanism with effective Regge parameter $\alpha_{eff} \simeq 0$ At small t this contribution may be interpreted in terms of one pion exchange diagram (Fig. 8)

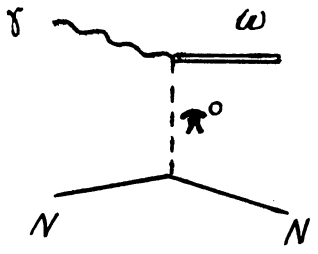

Fig. 8 Feynman diagram for the one pion exchange in the ω-production.

The t-dependence of $d\sigma(\gamma p \to \rho^0 p)$ and $d\sigma(\gamma p \to \varphi p)$ is shown in Fig. 9. The solid curves correspond to the formulae

$$d\sigma(\gamma p \to \rho^0 p) = C_\rho \left[\sqrt{d\sigma(\pi^+ p \to \pi^+ p)} + \sqrt{d\sigma(\pi^- p \to \pi^- p)}\right]^2 \qquad (4.13)$$

$$d\sigma(\gamma p \to \varphi p) = C_\varphi \left[\sqrt{d\sigma(K^+ p \to K^+ p)} + \sqrt{d\sigma(K^- p \to K^- p)} - \sqrt{d\sigma(\pi^- p \to \pi^- p)}\right]^2 \qquad (4.14)$$

which have been obtained within the framework of additive quark model and assuming, that the spin effects in the quark--quark and quark-antiquark scattering are insignificant at high energies. The last assumption enables us to express $\langle V'N | VN \rangle$ - amplitudes in (4.II) through the pseudoscalar - meson - nucleon scattering amplitudes. Eqs.(4.I3)

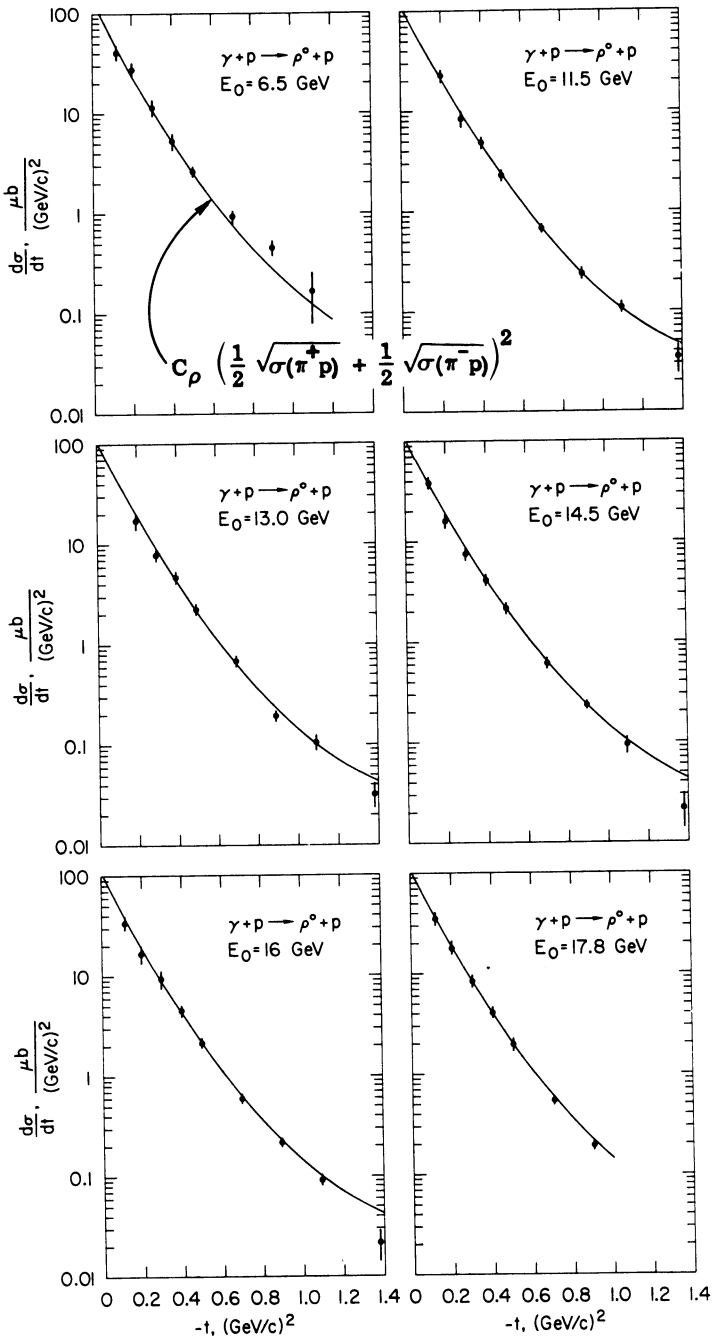

Fig. 9a Comparison of the VMD and quark model predictions with high-energy ρ^0 photoproduction. (From Ref. 13).

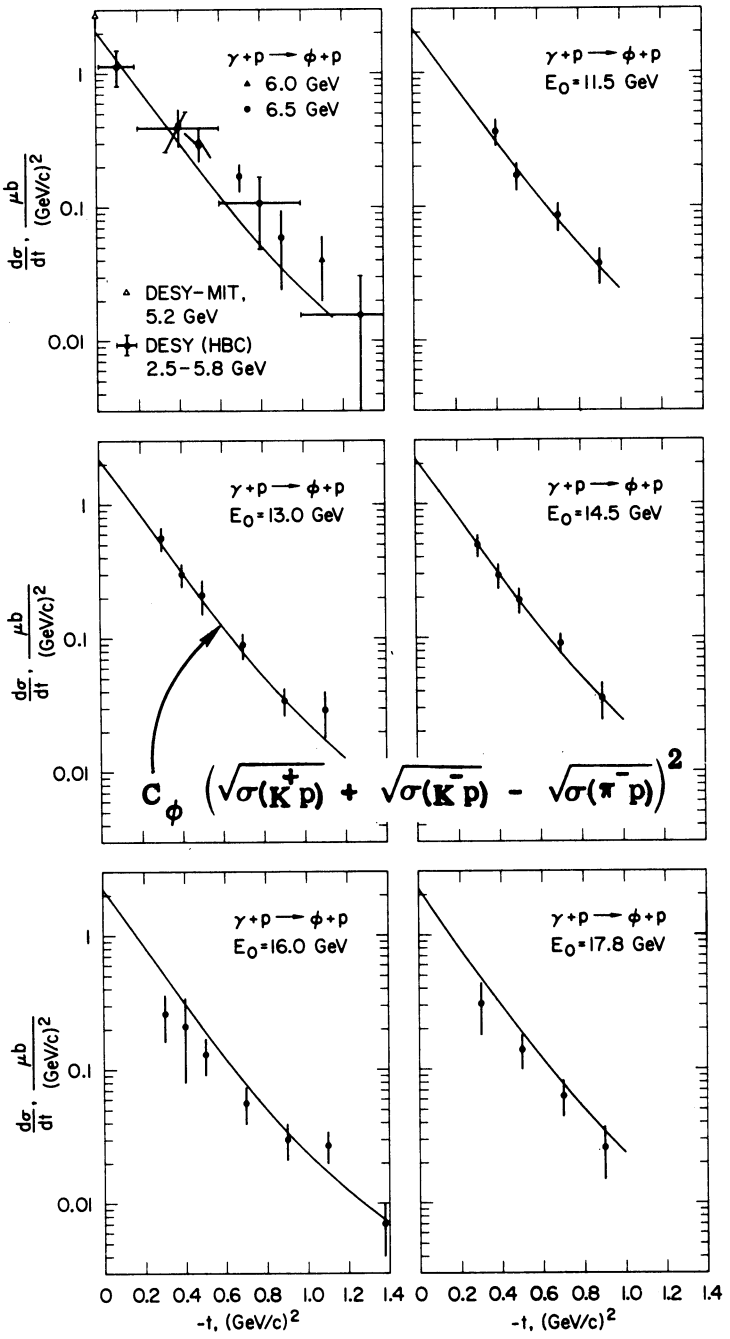

Fig. 9b Comparison of the VMD and a broken SU(3) quark model predictions with ϕ photoproduction. (From Ref. 13).

and (4.I4) are seen in Fig. 7 and 8 to fit the data extremely well.

The spin dependence of $T(\gamma N \to VN)$ can be studied via the decay angular distribution of the vector mesons produced by the unpolarized as well as polarized photons. Let us consider the reaction $\gamma p \to \rho^0 p \to \pi^+\pi^- p$. The decay angular distribution of pions in the ρ^0 rest frame is described by the standard formula

$$\frac{dN}{d\cos\theta d\varphi} \equiv W(\theta,\varphi) = \hat{M}\rho(V)\hat{M}^{+} = \sum_{\lambda_V \lambda'_V} \langle \theta,\varphi|M|\lambda_V\rangle \rho_{\lambda_V \lambda'_V} \times \langle \lambda'_V|M^{+}|\theta,\varphi\rangle \qquad (4.I5)$$

where M is the decay amplitude of $\rho \to 2\pi$ with a given helicity state (or the polarization state) of the ρ -meson

$$\langle \theta,\varphi|M|\lambda_V\rangle = D\sqrt{\frac{3}{4\pi}}\, Y^{*}_{1,\lambda_V}(\theta,\varphi)$$

$$Y_{1,0}(\theta,\varphi) = \cos\theta$$

$$Y_{1,\pm 1}(\theta,\varphi) = \mp\frac{1}{\sqrt{2}}\sin\theta\, e^{\pm i\varphi} \qquad (4.I6)$$

The quantity $|D|^2$ is proportional to the ρ^0 decay width and is of no importance for the angular distribution analysis, since it is independent of λ_V due to the rotation invariance. The decay angles θ and φ are defined as the polar and azimuthal angles of the unit vector $\hat{n}$, which denotes the direction of flight of one of the pions in the ρ^0 rest frame (see Fig. 10). Using Eq.(4.I6) and averaging Eq.(4.I5) over φ , we get the angular distribution of ρ^0's , produced by the unpolarized γ's :

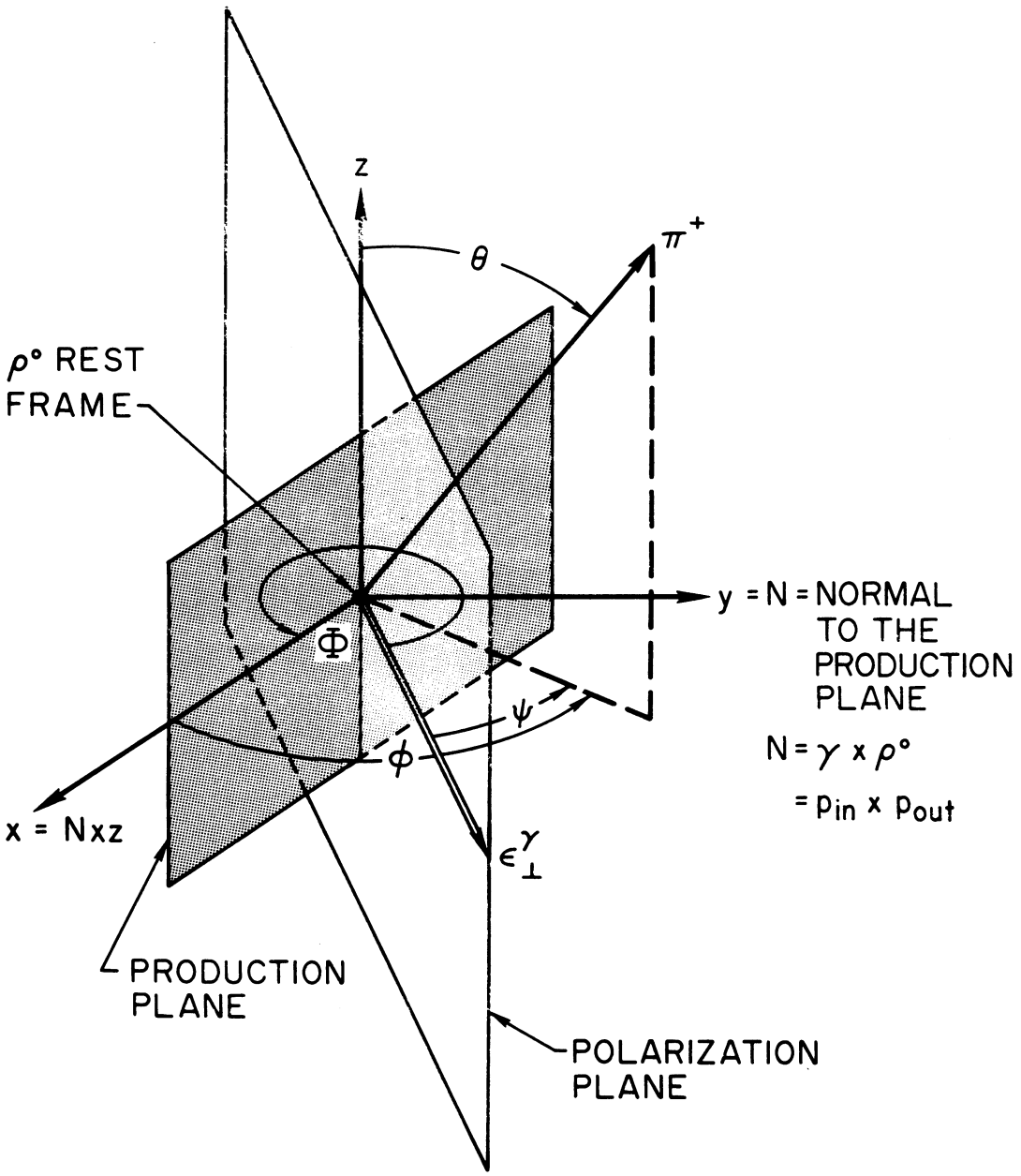

Fig. 10 Frame of reference used in analysis of the vector meson decays.

$$W(\theta) \sim \tfrac{1}{2}(\rho_{11}+\rho_{-1-1})\sin^2\theta+\rho_{00}\cos^2\theta = \\ = \rho_{11}\sin^2\theta + \rho_{00}\cos^2\theta \qquad (4.17)$$

Fig. 11 shows the distribution of the polar angle θ, which is proportional to $\sin^2\theta$. Thus, the rho mesons are produced predominantly in the transverse polarization states i.e. with c.m.s. helicity ± 1.

The forward photoproduction amplitude has, therefore, a form similar to that of the forward Compton scattering

$$f(\gamma N \to \rho^0 N) \simeq f_1(\omega)(\vec{\epsilon}_\gamma \cdot \vec{\epsilon}_\rho^{\,*}) + i(\vec{\sigma}\cdot[\vec{\epsilon}_\gamma \times \vec{\epsilon}_\rho^{\,*}])f_2(\omega) \ . \qquad (4.18)$$

In the case of the linearly polarized photons the pion decay angular distribution depends on mutual orientation of the photon polarization vector and the decay plane (or, equivalently the rho polarization vector). We consider only the case of the forward photoproduction of the transverse polarized rho-mesons.

There are here two limiting cases.

a) $\vec{\epsilon}_\rho \parallel \vec{\epsilon}_\gamma$. As seen in Fig. 10, Φ is the angle of the photon electric polarization vector with respect to the production plane. Since we consider the case of $\vec{\epsilon}_\rho \parallel \vec{\epsilon}_\gamma$ we have

$$|\vec{\epsilon}(\rho)\rangle = -\frac{1}{\sqrt{2}}\left(e^{+i\Phi}|\lambda_\rho = +1\rangle - e^{-i\Phi}|\lambda_\rho = -1\rangle\right) \qquad (4.19)$$

Now, after substitution of Eq.(4.19) into Eq.(4.15) and making use of (4.16), we obtain

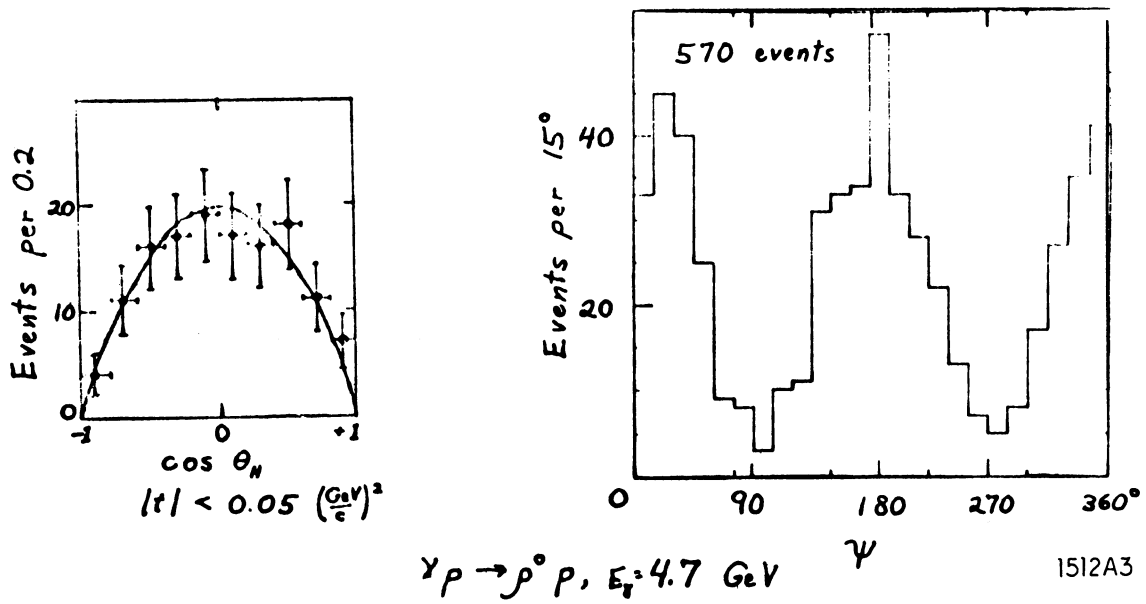

Fig. 11 Angular distributions for the decays of ρ^0 produced by polarized and unpolarized photons. (From Ref. 13)

$$W_{\parallel}(\theta,\varphi,\Phi) \sim \sin^2\theta \cos^2\psi \qquad (4.20)$$

where $\psi = \varphi - \Phi$ is the azimuthal angle with respect to the photon polarization plane.

b) If $\vec{\epsilon}_\rho \perp \vec{\epsilon}_\gamma$, then

$$W_{\perp}(\theta,\varphi,\Phi) \sim \sin^2\theta \sin^2\psi \qquad (4.21)$$

with the same notations.

The experimental ψ -distribution is proportional to $\cos^2\psi$ (see Fig. 11) and show that the rho is tending to "conserve" the direction of the photon polarization i.e. it is almost completely linearly polarized. This means also, that $|f_1| \gg |f_2|$ in Eq.(4.18) and

$$\left.\frac{d\sigma}{d\Omega}\right|_{0^\circ}(\gamma N \to \rho_0 N) \simeq |f_1|^2 = (Im\, f_1)^2 (1+\alpha_\rho^2)$$
$$\alpha_\rho = \frac{Re\, f_1}{Im\, f_1} \qquad (4.22)$$

According to VMD - relations (4.II) we can write now [20]

$$\sigma_{tot}(\gamma p) = \frac{4\pi}{\omega} Im\, f_1(\gamma p \to \gamma p) \simeq \frac{4\pi}{\omega} \sum_{V=\rho,\omega,\varphi} g_{\gamma V} \sqrt{\frac{d\sigma}{d\Omega}(\gamma p \to V p)_{0^\circ}} \qquad (4.23)$$

The comparison of Eq.(4.23) with experiment is shown in Fig. 12 and is found to be good, [13] if the $g_{\gamma V}$'s are taken from the storage ring data on the vector meson production in the electron-positron annihilation (see the last Section of the notes).

One can test also Eq.(4.23) (with quite an evident modification) in the photon-nucleus reactions. Of special interest here is the atomic number dependence of the corres-

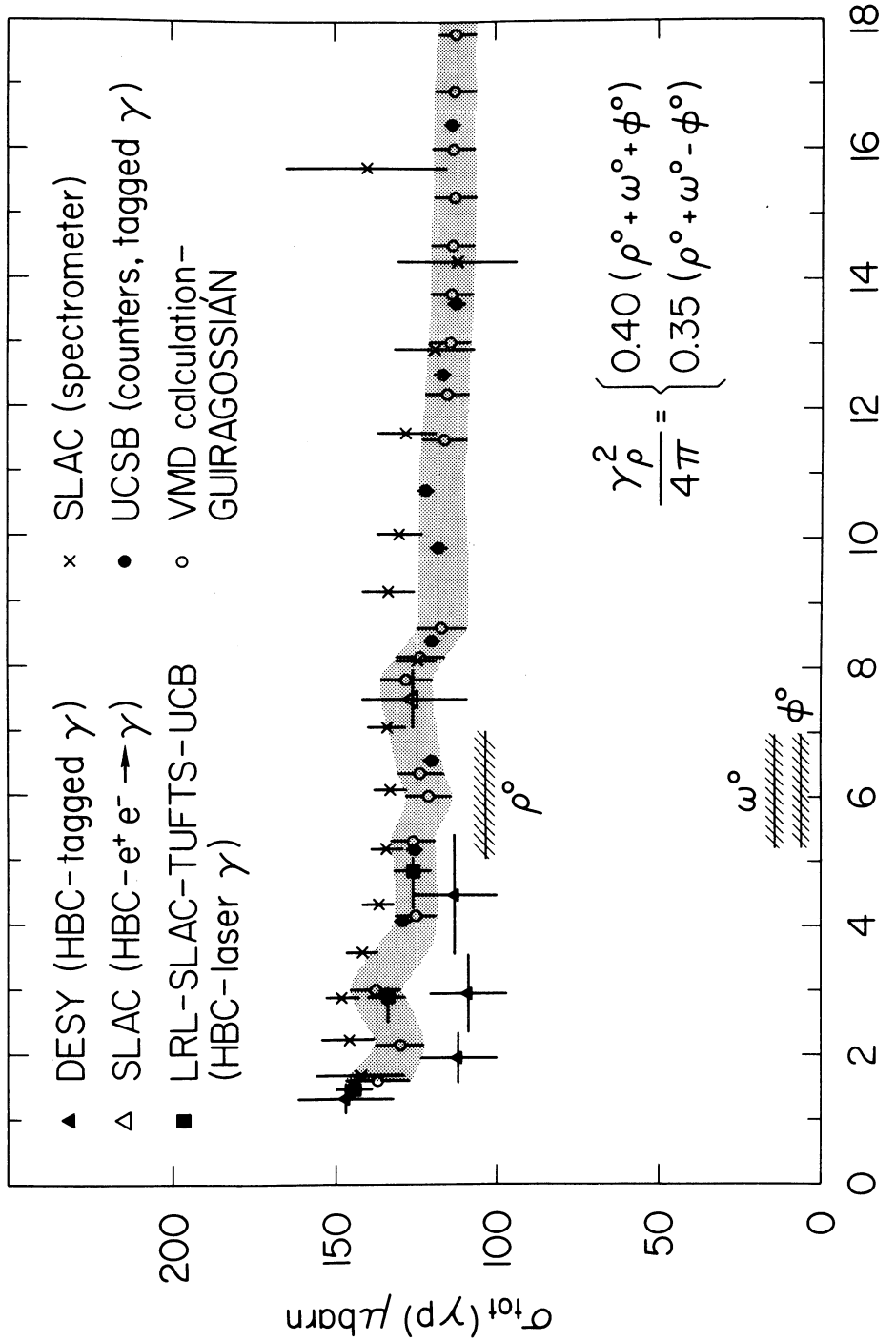

Fig. 12 Comparison of the VMD predictions for $\sigma_{tot}(\gamma p)$ with experimental data. (From Ref. 13).

ponding cross sections:

$$\frac{d\sigma}{dt}(\gamma A \to V^0 A) = \frac{d\sigma}{dt}(\gamma N \to V^0 N) F^2(t),$$
$$F(0) = N_{eff}, \qquad (4.24)$$
$$\sigma_{tot}(\gamma A) = \sigma_{tot}(\gamma N) \cdot N_{eff}$$

Due to the multiple scattering of the produced V-mesons inside the nucleus one gets $N_{eff} < A$.[21]

The experimental data on $\sigma_{tot}(\gamma A)$ for a number of nuclei are shown in Fig. 13 and they tell us that some shadowing indeed takes place:

$$\frac{\sigma_{\gamma A}}{\sigma_{\gamma N}} \sim A^{0,8 \div 0,9} \qquad (4.25)$$

At very high energies the A-dependence of $\sigma_{tot}(\gamma A)$ should be the square root of that for the coherent ρ^0-production. It would be very interesting to test this VMD - prediction in the multi-GeV energy region.

The coherent ρ^0-production on complex nuclei is sensitive to the real part of the "elementary" interaction amplitude $f(\gamma N \to \rho^0 N)$, to the hadron matter distribution inside the nucleus, to the value and energy variation of $\sigma_{tot}(\rho N)$ and to the nucleon correlations. All these factors were taken into account by the DESY - group, who conclude from their analysis[22] that there is no significant disagreement between VMD and data on the ρ^0-photoproduction from complex nuclei. However, the situation has not yet found its final settlement, because there are disagreements between the results of various groups.[19]

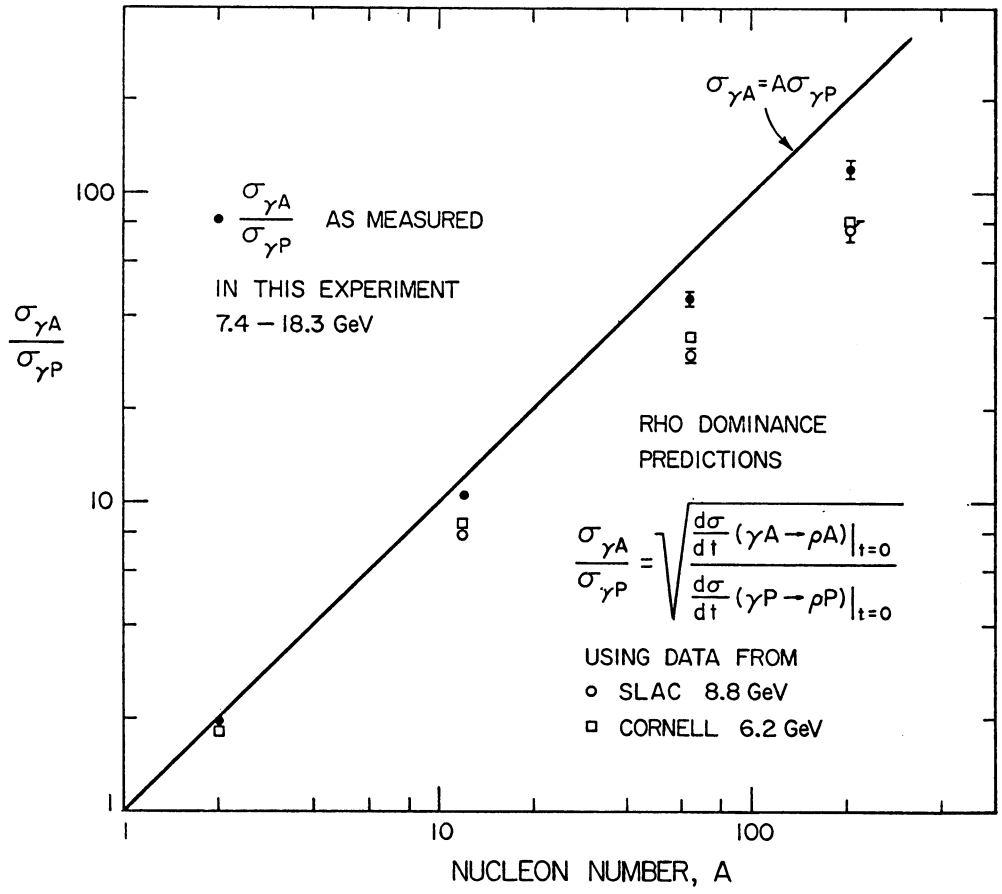

Fig. 13 Total γA cross-sections compared with $\sigma(\gamma A) = A\sigma(\gamma p)$ and with the VMD predictions using the Cornell and the SLAC ρ^0-photoproduction data. (From Ref. 26).

4.3 VMD and the pion photoproduction [23,24]

The general characteristics of photoproduction of pseudoscalar mesons at small t-values are shown in Fig. 14 and summarized in Table 6 [25,26].

Table 6

General features of pseudoscalar meson photoproduction

Region.	Features	Energy dependence
$\|t\| < 0,3$	Peaks and dips. Variations among different reactions.	No shrinkage $\frac{d\sigma}{dt} \sim K_\gamma^{-2}$
$\|t\| \simeq 0,5$	Dip in $\gamma N \to \pi^0 N$. "Smooth" t-dependence in all other reactions.	—"—
$\|t\| > 0,7$	Great similarity among reactions. Approximate exp(3t) - behaviour.	—"—
Small u.	Great similarity among reactions. No dips.	No shrinkage $\frac{d\sigma}{du} \sim K_\gamma^{-3}$

It is difficult to explain all these features on the basis of simple exchange models, especially the fact of approximate constancy of $K_\gamma^2 \frac{d\sigma}{dt}$ in energy for the entire t-region considered. In the Regge-pole language this fact would mean, that the "effective" Regge trajectory is the same for all processes and $\alpha_{eff}(t) \simeq 0$ for all $|t| < I,5\ GeV^2$. So much the greater interest is to compare the photoproduction cross sections with their corresponding hadronic counterparts, according to VMD.

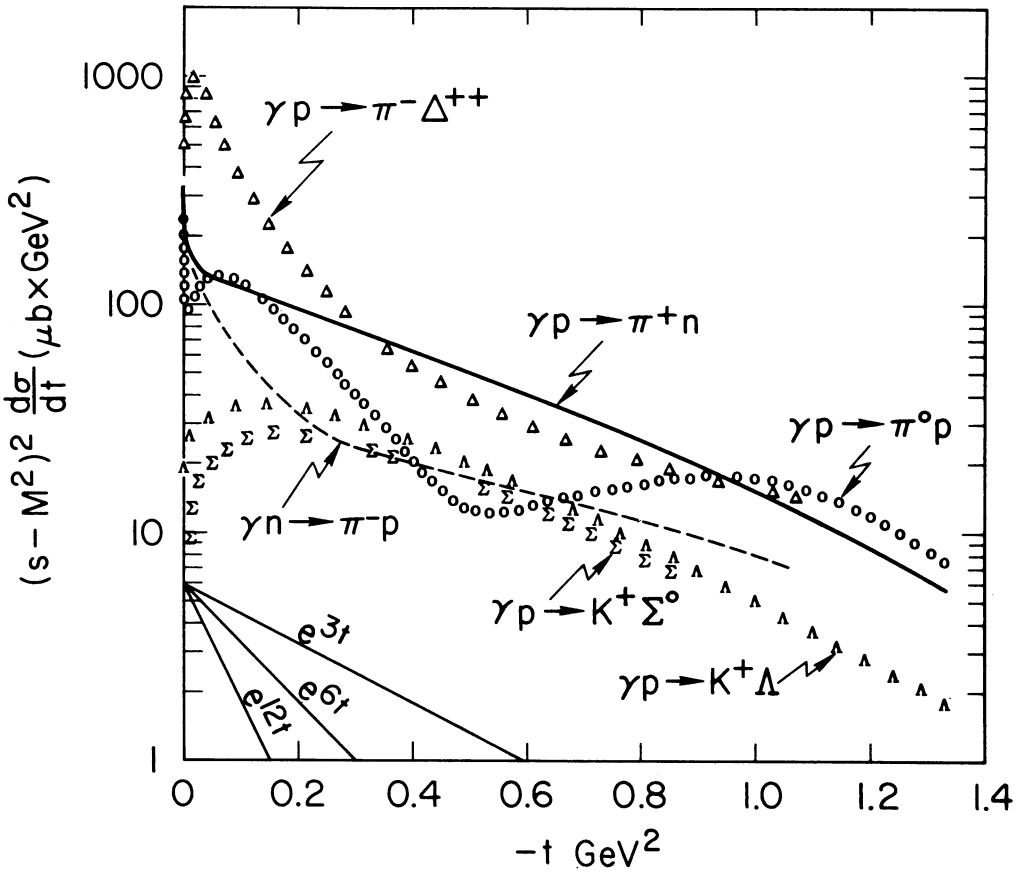

Fig. 14 Momentum-transfer dependence for various processes of pseudoscalar-meson photoproduction. (From Ref. 26).

We shall confine ourselves to discussion of the pion photoproduction cross sections which are the best known. From our basic formula (4.3) we get

$$\frac{d\sigma}{dt}(\gamma^{v}p\to\pi^{+}n)=g^{2}_{\gamma\rho}\frac{d\sigma}{dt}(\rho^{o}_{tr}\rho\to\pi^{+}n)=\frac{1}{2}g^{2}_{\gamma\rho}\frac{d\sigma}{dt}(\pi^{+}n\to\rho^{o}_{tr}\rho)$$
$$=g^{2}_{\gamma\rho}\cdot\frac{1}{2}\cdot(\rho_{11}+\rho_{-1-1})\frac{d\sigma}{dt}(\pi^{-}p\to\rho^{o}n)=g^{2}_{\gamma\rho}\rho_{11}(s,t)\frac{d\sigma}{dt}(\pi^{-}p\to\rho^{o}n) \qquad (4.26)$$

where symbol γ^{v} serves to specify only the transitions brought about by the isovector part of e.m. current.

In derivation of Eq.(4.26) we have used the relation between the direct and inverse reactions, which follow from T-invariance, as well as the isotopic invariance of the strong interactions. Furthermore, we have neglected the difference of the phase volumes and normalization factors of vector meson ($m_{v} \neq 0$) and photon ($m_{\gamma} = 0$), which are insignificant at $s \gg m^{2}_{\rho}$. The combination of the π^{+} - and π^{-} photoproduction on nucleons, which does not include the interference terms between the isovector and isoscalar part of e.m. current is most convenient to compare with experiment:

$$\frac{1}{2}\left(\frac{d\sigma}{dt}(\gamma p\to\pi^{+}n)+\frac{d\sigma}{dt}(\gamma n\to\pi^{-}p)\right)=\sum_{V=\rho,\omega,\varphi}g^{2}_{\gamma v}\rho_{11}(V)\frac{d\sigma}{dt}(\pi^{-}p\to Vn)+$$
$$+2g_{\gamma\omega}g_{\gamma\varphi}\,\mathrm{Re}\left[T^{*}(\omega_{tr}\rho\to\pi^{+}n)T(\varphi_{tr}p\to\pi^{+}n)\right]\simeq g^{2}_{\gamma\rho}\rho_{11}(\rho^{o})\frac{d\sigma}{dt}(\pi^{-}p\to\rho^{o}n) \qquad (4.27)$$

We have neglected the ω -and φ -contributions for the value of $\sigma(\pi p\to\varphi n)$ is very small and also due to the relation of the vector-meson-photon coupling constants

$$g^{2}_{\gamma\rho}:g^{2}_{\gamma\omega}:g^{2}_{\gamma\varphi}=9:1:2 \qquad (4.28)$$

following from the SU(6) - symmetry (or quark model) and fitting rather well to available data (see Table 8 in Section 6).

The main difficulty in the checking of Eq.(4.27) is that it is impossible to define in a relativistically invariant manner the vector meson state with $m_V^2 \neq 0$ and the transverse polarization. The subsidiary Lorentz condition (4.6) projects out linearly independent space-like vectors $\epsilon_\mu^{\lambda=1,2,3}$, which form the complete basis in the spin space of vector particle (with unit spin). Two "transverse" vectors $\epsilon_\mu^{\lambda=1,2}$ do not form the complete basis. Hence, even if the vector ϵ_μ is the transverse one in a given Lorentz frame, in some other frame it will have non-zero longitudinal component. Only in the limit $m_V \to 0$ the vector particle has two polarization states in any Lorentz frame. It is worthwhile to note in this connection, that in reactions of the vector meson production by pions on the (pseudo) scalar target, which does not change its internal parity

$$\pi + 0^\pm \to V + 0^\pm \qquad (4.29)$$

no problem of the projecting of the transverse polarization exists. The vector particle in (4.29) is automatically produced in the "photon-like" state due to the angular momentum and parity conservation.[27)]

Practically, the test of VMD relation

$$\frac{d\sigma}{dt}(\gamma He^4 \to \pi^0 He^4) = g_{\gamma\rho}^2 \frac{d\sigma}{dt}(\pi^\pm He^4 \to \rho^\pm He^4)$$

looks most promising. An additional advantage of this reac-

tion is that owing to the isoscalar property of the target only the isovector part of e.m. current operates. Hence, no problem of the ρ-ω interference arises.

In the case of reaction $\pi N \to \rho N$ the dynamical problem consists in determination of the reference frame, such that the trasverse elements ρ_{ij} $(i, j = \pm 1)$ of the spin density matrix were altered minimally under extrapolation $m_\nu \to 0$ and with fixed values of $s \gg m_\rho^2$ and $t \neq 0$. Theoretically, the question could be resolved within a reasonably simple model. The simplest one is the Born pole model (see Fig. 16)

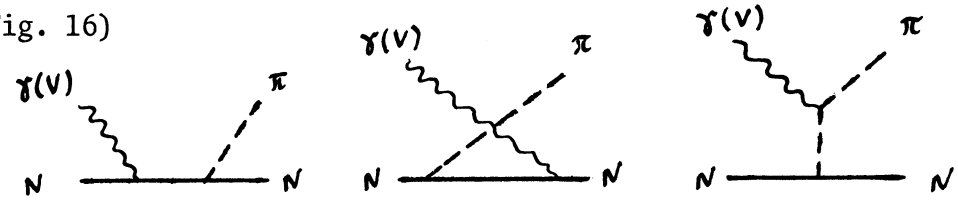

Fig. 15 Feynman diagrams of the Born approximation.

The predictions of the gauge-invariant pole models for $\gamma p \to \pi^+ n$ and also for $\gamma p \to \pi^- \Delta^{++}$ agree satisfactorily with experiment at $\sqrt{-t} \leq m_\pi$ (see Fig. 16 and 17). In particular, such characteristic qualitative features, as the sharp forward maximum (spike) in $\gamma p \to \pi^+ n$ and $\gamma n \to \pi^- p$ and the dip in the reaction $\gamma p \to \pi^- \Delta^{++}$ are reproduced quite well.

The calculation of the Feynman diagrams, shown in Fig. 15 can also be used for the theoretical analysis of the VMD formula (4.26). The following conclusions were obtained[28]:

I. Vector-meson dominance relation (4.26) must be tes-

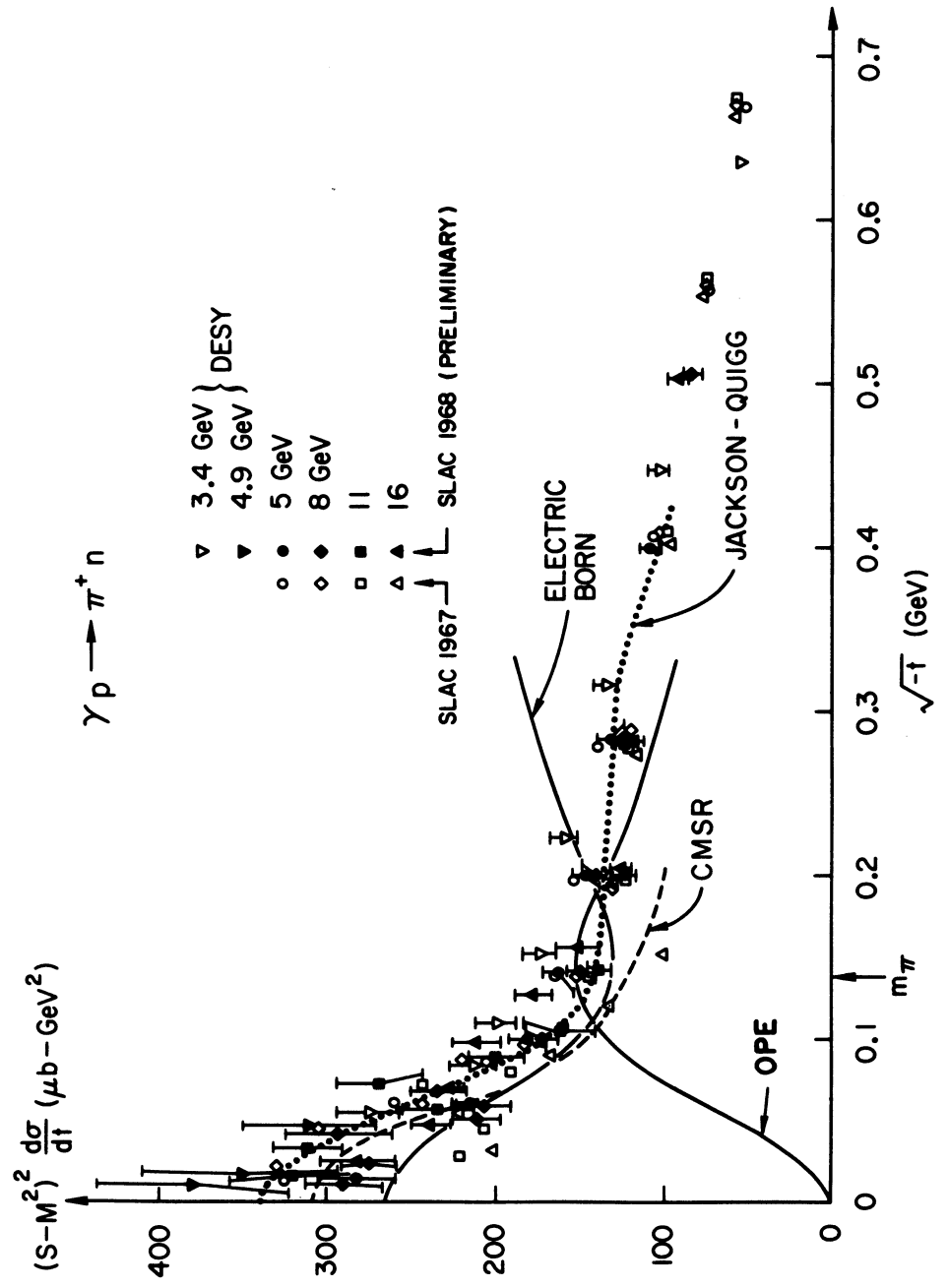

Fig. 16 Differential cross-section for π^+ photoproduction. (From Ref. 26).

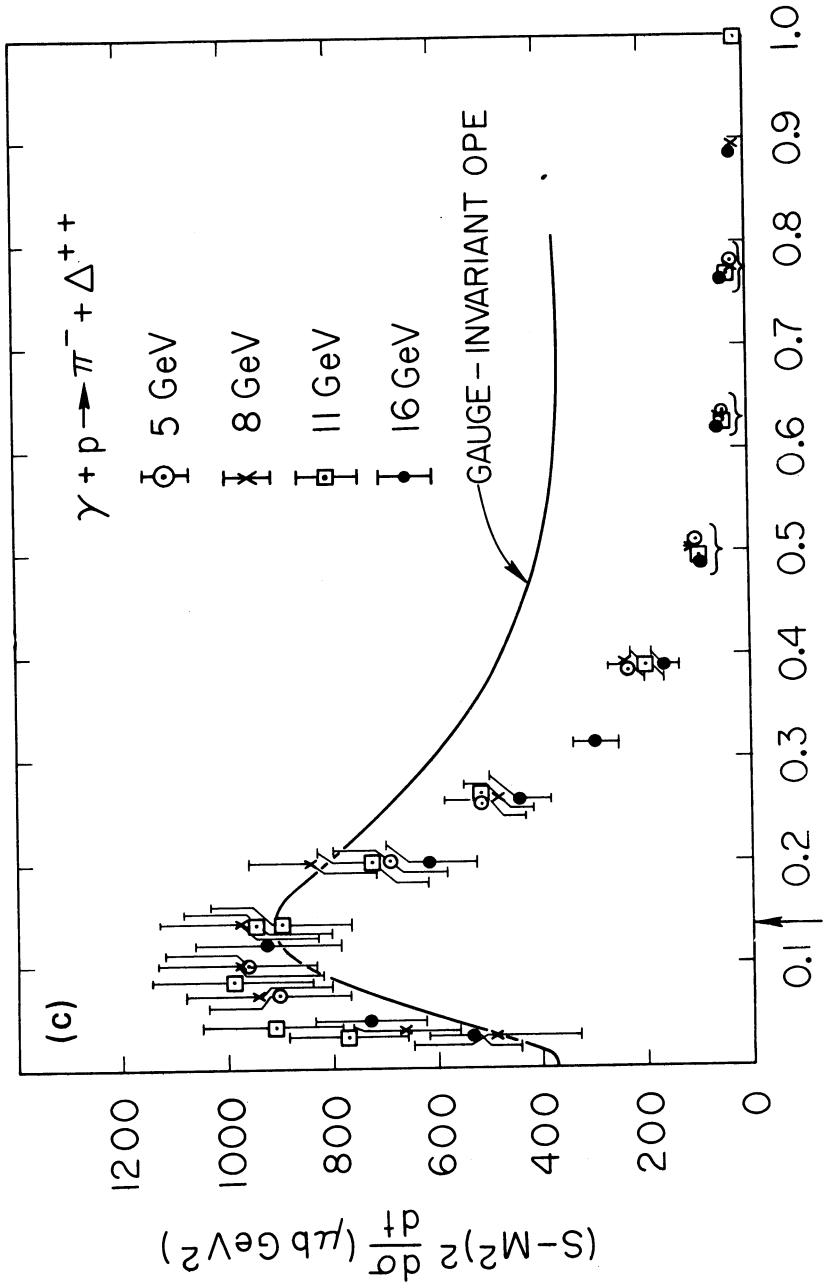

Fig. 17 Differential cross-section for Δ^{++} production. (From Ref. 26).

ted in the helicity frame i.e. the element $\rho_{11}^{H}(s,t)$ of the spin density matrix of rho-meson must be taken in the c.m.s. of the S-channel, when the spin quantization axis is directed along the rho-momentum in c.m.s.

2. The effect of $m_\rho \neq 0$ disappears for transversely polarized rho's as $s \to \infty$

3. At low energies relations (4.26) and (4.27) may be violated.

In full accordance with prescription of the point I) it was discovered recently that there exists the forward peak in $\rho_{11}^{H} \frac{d\sigma}{dt}(\pi^- p \to \rho^0 n)$ in the energy interval from 2,7 up to II,2 GeV.[29)]

The VMD gives the relation

$$\frac{d\sigma}{dt}(\gamma^v p \to \pi^0 p) = g_{\gamma\rho}^2 \rho_{11}^{H}(\rho^0) \frac{d\sigma}{dt}(\pi^0 p \to \rho^0 p) =$$

$$= \frac{1}{2} g_{\gamma\rho}^2 \left[\rho_{11}^{H}(\rho^+) \frac{d\sigma}{dt}(\pi^+ p \to \rho^+ p) + \rho_{11}^{H} \frac{d\sigma}{dt}(\rho^-) \frac{d\sigma}{dt}(\pi^- p \to \rho^- p) - \right.$$

$$\left. - \rho_{11}^{H}(\rho^0) \frac{d\sigma}{dt}(\pi^- p \to \rho^0 n) \right] \qquad (4.30)$$

Since $\frac{d\sigma}{dt}(\gamma p \to \pi^0 p)$ has dip at $t \simeq 0{,}5$ GeV^2, we must expect analogous dip in the linear combination of cross sections entering the right-hand side of Eq.(4.30). Remarkably enough, that this qualitative prediction of the VMD is also confirmed by experiment.[30)]

In Fig. 18 the check of Eq.(4.27) is shown in the range of $0 \leq \sqrt{|t - t_{min}|} \leq 0.8$ GeV. The agreement is reasonable. However, the VMD meets serious difficulties in the explanation of the experiments on pion photoproduction by linearly

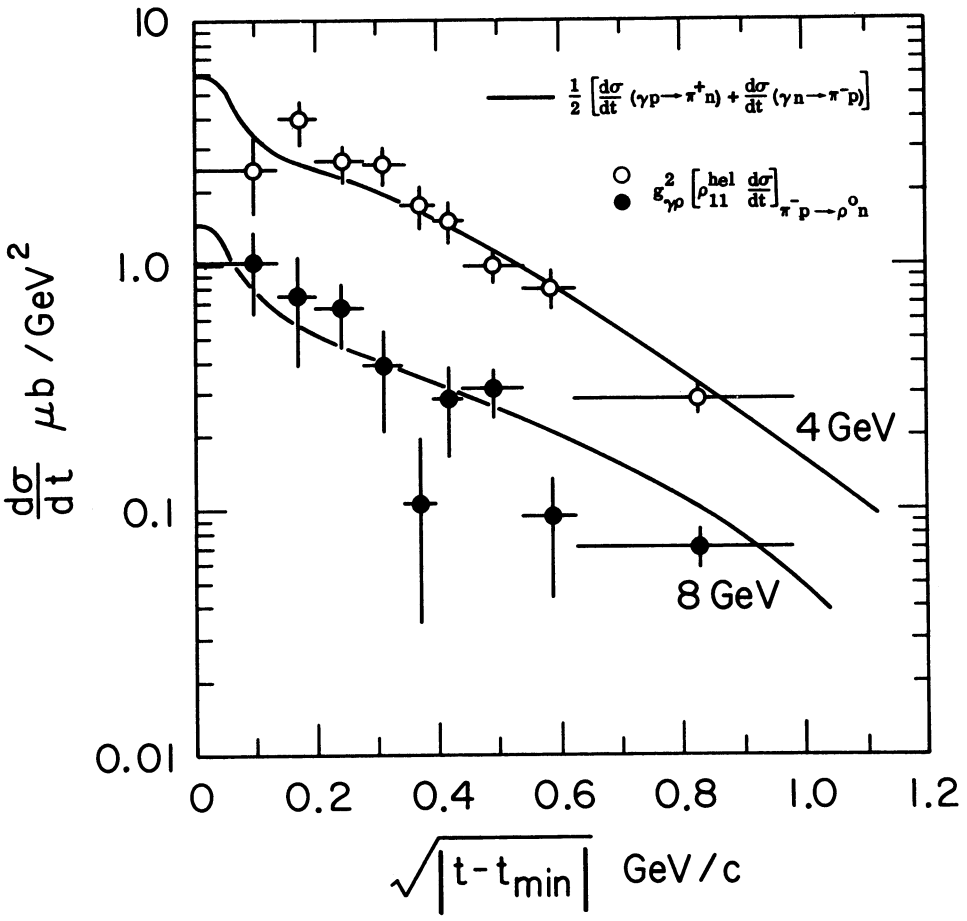

Fig. 18 The VMD comparison for single pions produced by unpolarized photons. (From Ref. 26).

polarized photons.

With definitions

$$\vec{\epsilon}(\lambda=\pm 1) = \mp \frac{1}{\sqrt{2}} (\vec{\epsilon}_x \pm i \vec{\epsilon}_y)$$

one readily obtains

$$\begin{aligned} d\sigma_\perp &= \rho_{11}\, d\sigma + \rho_{1-1}\, d\sigma \\ d\sigma_\parallel &= (\rho_{11} - \rho_{1-1})\, d\sigma \\ A &= \frac{d\sigma_\perp - d\sigma_\parallel}{d\sigma_\perp + d\sigma_\parallel} = \frac{\rho_{1-1}}{\rho_{11}} \end{aligned} \qquad (4.3I)$$

where $d\sigma_{\perp(\parallel)}$ is the pion production cross section by linearly-polarized photons with the polarization vector $\vec{\epsilon}_{\gamma\perp}$ or $\parallel$ to the reaction plane (If, for example, the reaction plane is the x - z plane, then $\vec{\epsilon}_\perp = \{0, I, 0\}$, $\vec{\epsilon}_\parallel = \{I, 0, 0\}$).

Table 7 summarizes the comparison of the VMD formula

$$A(\pi^+ + \pi^-) = \left. \frac{\rho^H_{1-1}}{\rho^H_{11}} \right|_{\pi^- p \to \rho^0 n} \qquad (4.32)$$

with experiment.[31]

T a b l e 7

t GeV^2	A_{VDM}(2,7 GeV)	A_{exp}(3.4GeV)	A_{VDM}(4 GeV)
-0,2	-0,06 ± 0.32	+0,62 ± 0.07	-0,28 ± 0.34
-0,4	-0,49 ± 0.35	+0,43± 0.08	-0,43 ± 0.37

The sharp disagreement of Eq.(4.32) with data may be explained to some extent by using too low values of the photon energies. But the main part of this disagreement is more likely due to the poorly determined $\rho^H_{1-1}(\rho^0)$ from the re-

action $\pi N \to 2\pi N$. The note was made,[32] that some admixture of d-wave in the π-π final state may result in a significant changing of $\rho^H_{1-1}(\pi^- p \to \rho^0 n)$.

In conclusion of this section we make a few remarks on possible application of VMD to the reactions $\gamma N \to \pi \Delta$ and $\pi N \to V \Delta$.

An additional assumption is needed here about approximate equalities of the matrix element modulus connected by $s \rightleftarrows u$ crossing symmetry, namely

$$|M(\gamma N \to \pi \Delta)| \simeq |M(\pi N \to \gamma \Delta)| \qquad (4.33)$$

While the asymptotic theorems underlying the differential cross section equality

$$\frac{d\sigma}{dt}(\gamma N \to \pi \Delta) \simeq \frac{d\sigma}{dt}(\pi N \to \gamma \Delta) \qquad (4.34)$$

are the direct consequences of very general properties of local field theory[33], they are valid only in the sense of limit $s \to +\infty$. Therefore, the violation of relation of the type

$$\frac{1}{2}\left[\frac{d\sigma}{dt}(\gamma p \to \pi^- \Delta^{++}) + \frac{d\sigma}{dt}(\gamma n \to \pi^+ \Delta^-)\right] \simeq$$
$$\simeq g^2_{\gamma\rho}\rho^H_{11}(\rho^0)\frac{d\sigma}{dt}(\pi^+ p \to \rho^0 \Delta^{++}) + g^2_{\gamma\omega}\rho^H_{11}(\omega)\frac{d\sigma}{dt}(\pi^+ p \to \omega \Delta^{++}) \qquad (4.35)$$

can always be related to insufficiently high energies, which are needed to validate the asymptotic theorems. All the same should be kept in mind when a comparison is made between the K-meson photoproduction from nucleons, $\gamma + N \to K + Y$, and the ρ^0, ω and φ-meson production in the reactions

$\bar{K} + N \rightarrow V + Y$.

To summarize, the application of VMD to correlation of the photoproduction data with pure hadronic reactions leads at least to the qualitative agreement with experiment. This fact means, that the photon behaves in the "hadron-like" manner in its interaction with the hadron matter. We have seen, that such general features as dips, peaks, slopes etc. of the photon reactions are very similar to those of the corresponding vector-meson production reactions. However, the precise quantitative test of VMD hypothesis is damaged heavily by present difficulties in separating the genuine resonance rho-production amplitudes from the non-resonant background.

5. BEHAVIOUR OF FORM FACTORS IN ELECTRON-NUCLEON SCATTERING.

5.I Kinematics.

We begin the discussion of the high energy electron-nucleon interaction with definition of kinematics of the general inelastic ep - scattering

$$e + p \rightarrow p + \text{anything}. \qquad (5.I)$$

The Feynman diagram of this process is shown in Fig. 19

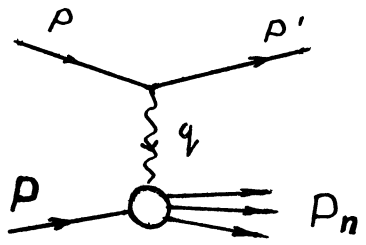

Fig. 19 Kinematics of inelastic electron-nucleon scattering.

The matrix element for the reaction presented in Fig. 19 is

$$T = \frac{4\pi\alpha}{q^2} \langle p' | j^{\mu}(0) | p \rangle \langle p_n | J_{\mu}(0) | p \rangle (2\pi)^4 \delta^{(4)}(p+q-p_n) \quad (5.2)$$

We consider the case when the inelastically scattered electron only is detected. The differential cross section averaged over the initial proton and electron spin and summed over all final hadronic states is of the form

$$\frac{d^2\sigma}{d\varepsilon' d\Omega'} = \frac{2\alpha^2}{q^4} \cdot \frac{\varepsilon'}{\varepsilon} \cdot (p_\mu p'_\nu + p'_\mu p_\nu + \tfrac{1}{2} q^2 g_{\mu\nu}) W_{\mu\nu} \quad (5.3)$$

The tensor structure of $W_{\mu\nu}$ (an average over the nucleon spin is understood)

$$W_{\mu\nu} = (2\pi)^3 \sum \langle p | J_\mu(0) | p_n \rangle \langle p_n | J_\nu(0) | p \rangle \delta^{(4)}(p+q-p_n), \quad (5.4)$$

by Lorentz and gauge invariance can be written as

$$W_{\mu\nu} = W_1 \left(-g_{\mu\nu} + \frac{q_\mu q_\nu}{q^2}\right) + W_2 \left(p_\mu - \frac{p\cdot q}{q^2} q_\mu\right)\left(p_\nu - \frac{pq}{q^2} q_\nu\right) \frac{1}{M^2} \quad (5.5)$$

where $W_i = W_i(\nu, q^2)$ $(i = I, 2)$ are the functions of only two scalar quantities

$$\nu = q_0 = \varepsilon - \varepsilon' = \frac{q\cdot p}{M}, \qquad -q^2 = -(p-p') = 4\varepsilon\varepsilon' \sin^2\frac{\theta}{2}. \quad (5.6)$$

We shall neglect everywhere the lepton mass: $m_e^2 \ll \varepsilon^2$, $\vec{p}_e^{\,2} \simeq \varepsilon^2 (\vec{p}_e'^{\,2} = \varepsilon'^2)$.

After substitution of Eq.(5.5) into Eq.(5.3) we have [34]

$$\frac{d^2\sigma}{d\varepsilon' d\Omega'} = \frac{4\alpha^2}{q^4} \varepsilon'^2 \left[W_2(\nu, q^2) \cos^2\frac{\theta}{2} + 2W_1(\nu, q^2) \sin^2\frac{\theta}{2}\right] \quad (5.7)$$

Let us choose the frame of reference specified by $P = (M, 0, 0, 0)$ and $q_\mu = (q_o, 0, 0, q_z)$ and define the excitation cross sections of nucleon by the transverse and longitudinal virtual photons through equations

$$\sigma_\perp \equiv \sigma_t = \frac{4\pi^2\alpha}{K} W_{xx} = \frac{4\pi^2\alpha}{K} W_{yy} \tag{5.8}$$

$$\sigma_\parallel = \frac{4\pi^2\alpha}{K} W_{zz} \tag{5.9}$$

$$K = \frac{W^2 - M^2}{2M} = \frac{(P+q)^2 - M^2}{2M} = \nu + \frac{q^2}{2M} \tag{5.10}$$

where K is the equivalent photon energy for photoproduction with real photons of the final hadronic state with invariant mass of W.

From the definitions (5.5), (5.8) and (5.9) it follows

$$W_1 = \frac{K}{4\pi^2\alpha} \sigma_t \ , \tag{5.11a}$$

$$W_2 = -\frac{q^2}{\nu^2 - q^2} \cdot \frac{K}{4\pi^2\alpha} (\sigma_t + \sigma_s), \tag{5.11b}$$

$$\sigma_s \equiv -\frac{q^2}{\nu^2} \sigma_\parallel \equiv \sigma_\ell \tag{5.11c}$$

and, finally, the Hand's representation [35]

$$\frac{d^2\sigma}{d\mathcal{E}' d\Omega'} = \Gamma_t (\sigma_t + \epsilon \sigma_s) \tag{5.12}$$

with

$$\Gamma_t = \frac{\alpha}{2\pi^2} \cdot \frac{K}{q^2} \cdot \frac{\mathcal{E}'}{\mathcal{E}} \cdot \frac{1}{1-\epsilon} \ , \tag{5.13a}$$

$$\epsilon = \left[1 + 2(1 - \nu^2/q^2) \tan^2 \frac{\theta}{2} \right]^{-1}. \tag{5.13b}$$

In the case of the elastic scattering ($W = M^2$) or excitation of the nucleon resonance with mass of M^*, the kinematical variables ν and q^2 are related to each other

$$\begin{aligned} 2M\nu &= -q^2 \\ 2M\nu &= -q^2 + M^{*} - M^2 \end{aligned} \qquad (5.14)$$

The corresponding differential cross sections are obtained from Eqs.(5.3) and (5.4) with the replacement $|p_n\rangle \to |N(N^*)\rangle$ and evaluation of the one-particle matrix elements of e.m. current. In general, the transition matrix element $N^* \rightleftharpoons N+\gamma$ is described by three form factors

$$f_\rho(q^2) \sim \langle N^*, \lambda' | J_\rho(0) | N, \lambda = 1/2 \rangle, \qquad (5.15)$$

$$\rho = +, -, 0,$$

$$J_\pm = -\frac{1}{\sqrt{2}} (J_x \pm i J_y). \qquad (5.16)$$

$$J_0 = \frac{q_z}{q_0} J_z, \qquad (5.17)$$

where λ and λ' are the helicities of nucleon and the nucleon resonance. (In Eq.(5.17) we have taken into account the current conservation requirement $q_\mu J_\mu = q_0 J_0 - q_z J_z = 0$).

The transverse form-factors $f_\pm$ can be expressed in terms of the electric and magnetic multipole amplitudes while f_0 describes the longitudinal (Coulomb) transitions.

We write down the explicit form only for the elastic scattering cross section

$$\frac{d\sigma}{d\Omega'} = \frac{4\alpha}{q^4} \varepsilon'^2 \cdot \frac{\varepsilon'}{\varepsilon} \left[\frac{G_E^2 + \tau G_M^2}{1+\tau} \cos^2\frac{\theta}{2} + 2\tau G_M^2 \sin^2\frac{\theta}{2} \right] \qquad (5.18)$$

where G_E and $G_M(q^2)$ are the nucleon charge and magnetic form factors, respectively, $\tau = -q^2/4M^2$. The relation between $G_{E,M}(q^2)$ and $F_{1,2}(q^2)$ is

$$G_E(q^2) = F_1(q^2) + \frac{q^2}{4M^2} F_2(q^2),$$
$$G_M(q^2) = F_1(q^2) + F_2(q^2) \qquad (5.19)$$

5.2 Experimental data.

The studies of elastic electron-nucleon scattering have dicovered two important facts:[36]

a) The nucleon form factors G_E and G_M satisfy approximately the "scaling law"

$$G_E^p = \frac{1}{\mu_p} G_M^p(q^2) = \frac{1}{\mu_n} G_M^N(q^2) = G_D(q^2)$$
$$G_E^N(q^2) = 0 \qquad (5.20)$$

b) The universal form factor $G_D(q^2)$ is closely approximated in a large region of $0 \leq -q^2 \leq 25$ GeV^2 by the dipole fit

$$G_D(q^2) = \left[1 - q^2/0.71\ GeV^2\right]^{-2} \qquad (5.21)$$

The departures from the scaling law (5.20) and the dipole formula (5.21) do not exceed $\pm$ 10 ÷ 15% in some particular intervals of q^2.[37]

In Fig. 20 the ratio $d\sigma_{inel}(ep \to eN^*)/d\sigma(ep \to ep)$ is shown for the excitation of nucleon resonances near 1236 MeV, 1525 MeV, 1690 MeV and 1950 MeV. These ratios rise at small threshold momentum transfer and stay approximately constant at $q^2 \gg 1$ GeV^2.[38]

Thus, we see, that both elastic cross section and that

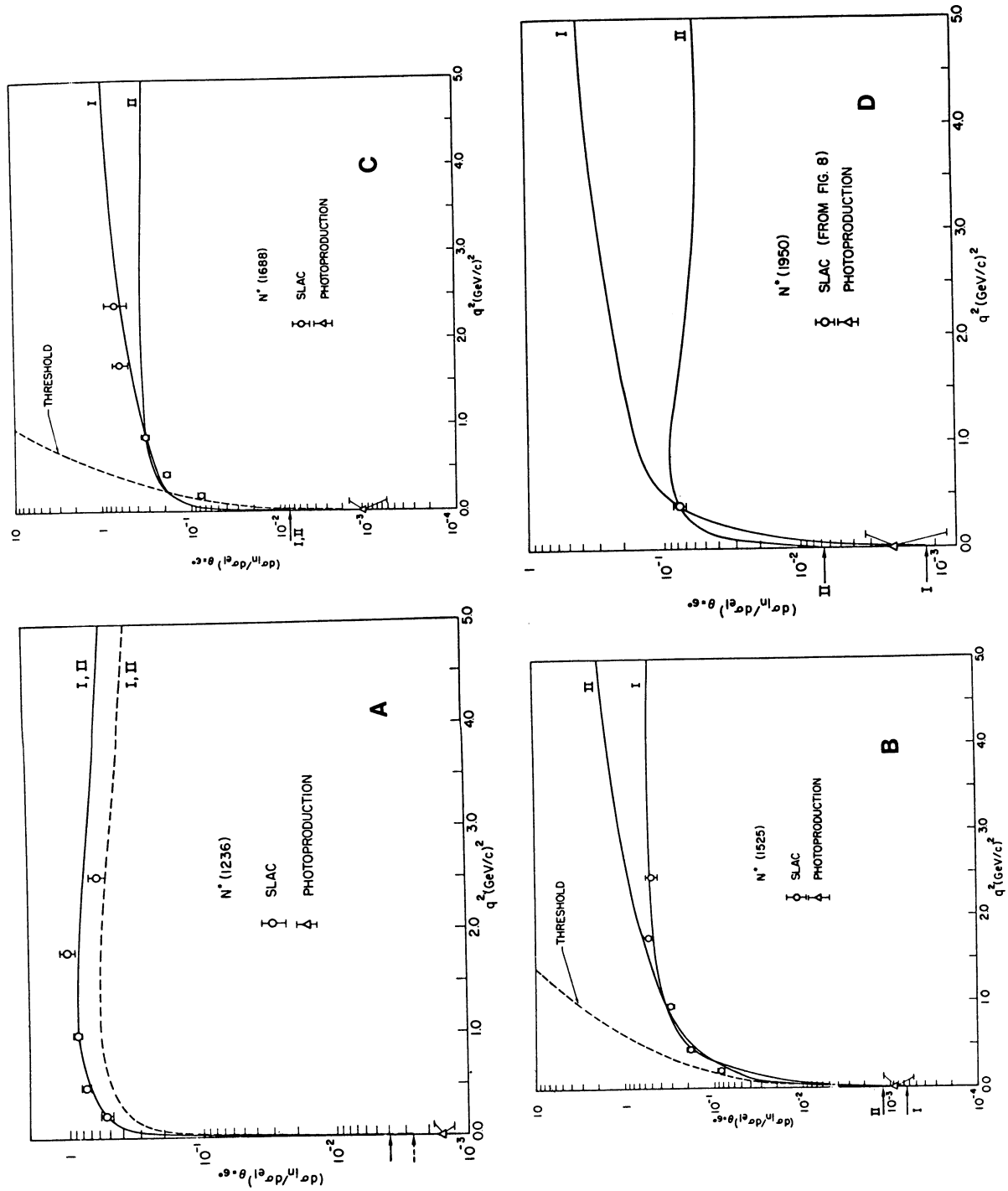

Fig. 20 Ratio of $d\sigma_{inel}(ep \to eN^*)/d\sigma_{el}(ep \to ep)$ plotted versus q^2. (From Ref. 13).

for the nucleon resonance excitation decrease rapidly with increasing q^2:

$$\frac{d\sigma}{d\Omega}(ep \to ep(N^*)) \sim \left(\frac{d\sigma}{d\Omega}\right)_{NS} G_D^2 \sim \frac{1}{q^8}\left(\frac{d\sigma}{d\Omega}\right)_{NS} \qquad (5.22)$$

where $(d\sigma/d\Omega)_{NS}$ stands for the elastic cross section for the point-like structureless proton.

The most interesting and exciting results were obtained in recent studies of the deep inelastic e-p scattering, when ν and q^2 take the large values.[39]

Fig. 21 shows, that in the region of $W \geqslant 2$ GeV the ratio of the experimental cross section to that from the point-like proton (the Mott cross section) goes down like q^{-2} instead of q^{-8}, according to Eq.(5.22).

In the experiments with only final electron detected, one can measure the ratio $R = \frac{\sigma_l}{\sigma_t}$, as is seen from Eqs. (5.I2) and (5.I3). At $|q^2| \geqslant I,5$ GeV^2 the value of R is consistent with zero and in any case it is less than 0,5. The dependence of R from ν and q^2 is seen to be rather weak. If one adopts, that $R = 0$ the value of $\nu W_2(\nu, q^2)$ displays the scaling property being a function of only ratio of $\omega = \frac{2M\nu}{q^2}$. All the data measured at various magnitudes of ν and q^2, but at fixed values of $\omega = \frac{2M\nu}{q^2}$ are situated on one and the same universal curve (see Fig. 22).

5.3 Theoretical models.

5.3.I. Elastic scattering.

It follows from Eqs.(5.20) and (5.2I) that the pole approximation of Eq.(4.4) of the vector meson dominance

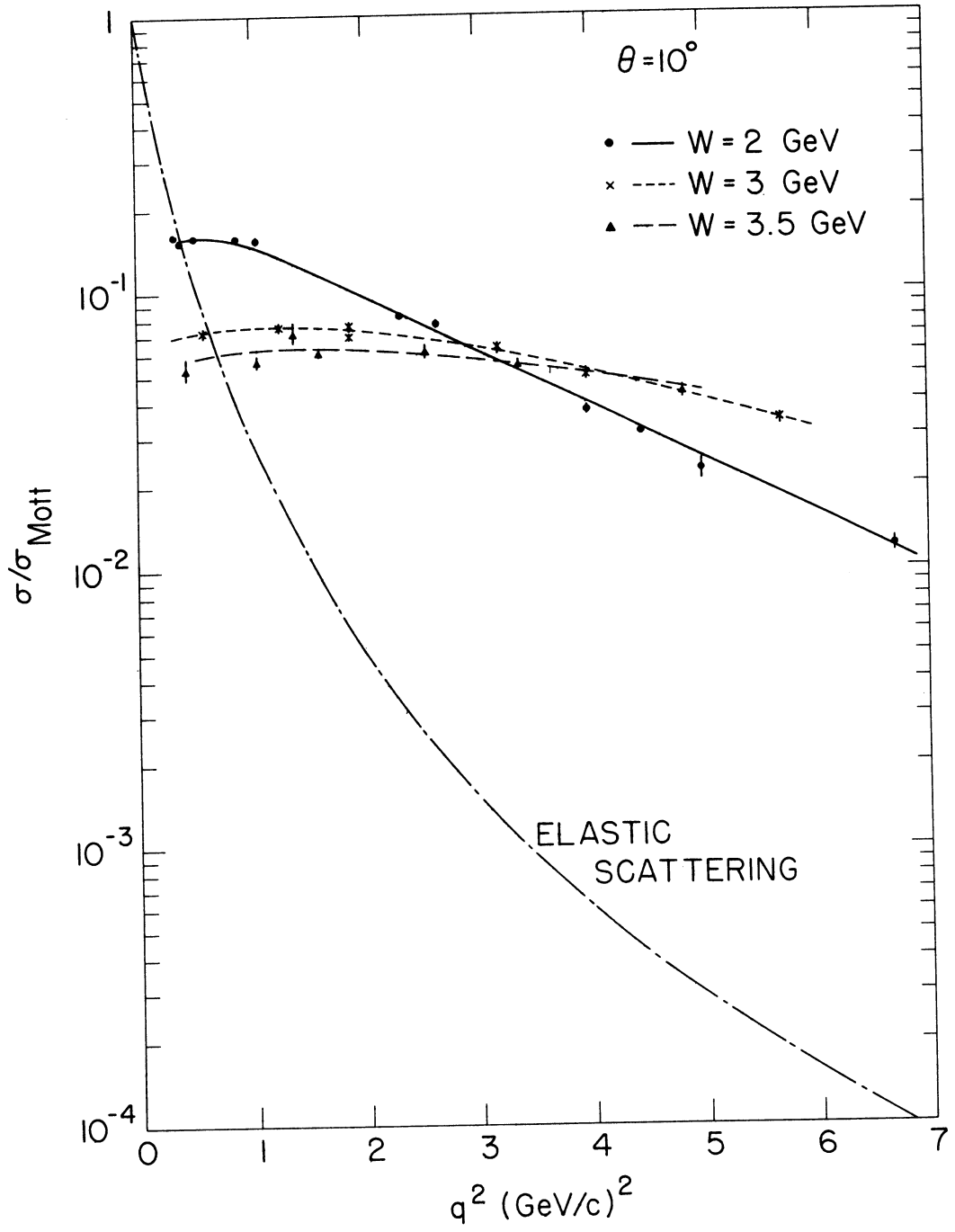

Fig. 21 Ratio of $d\sigma_{inel}(q^2,W)/d\sigma_{Mott}(q^2)$ plotted versus q^2 at fixed W. (From Ref. 39).

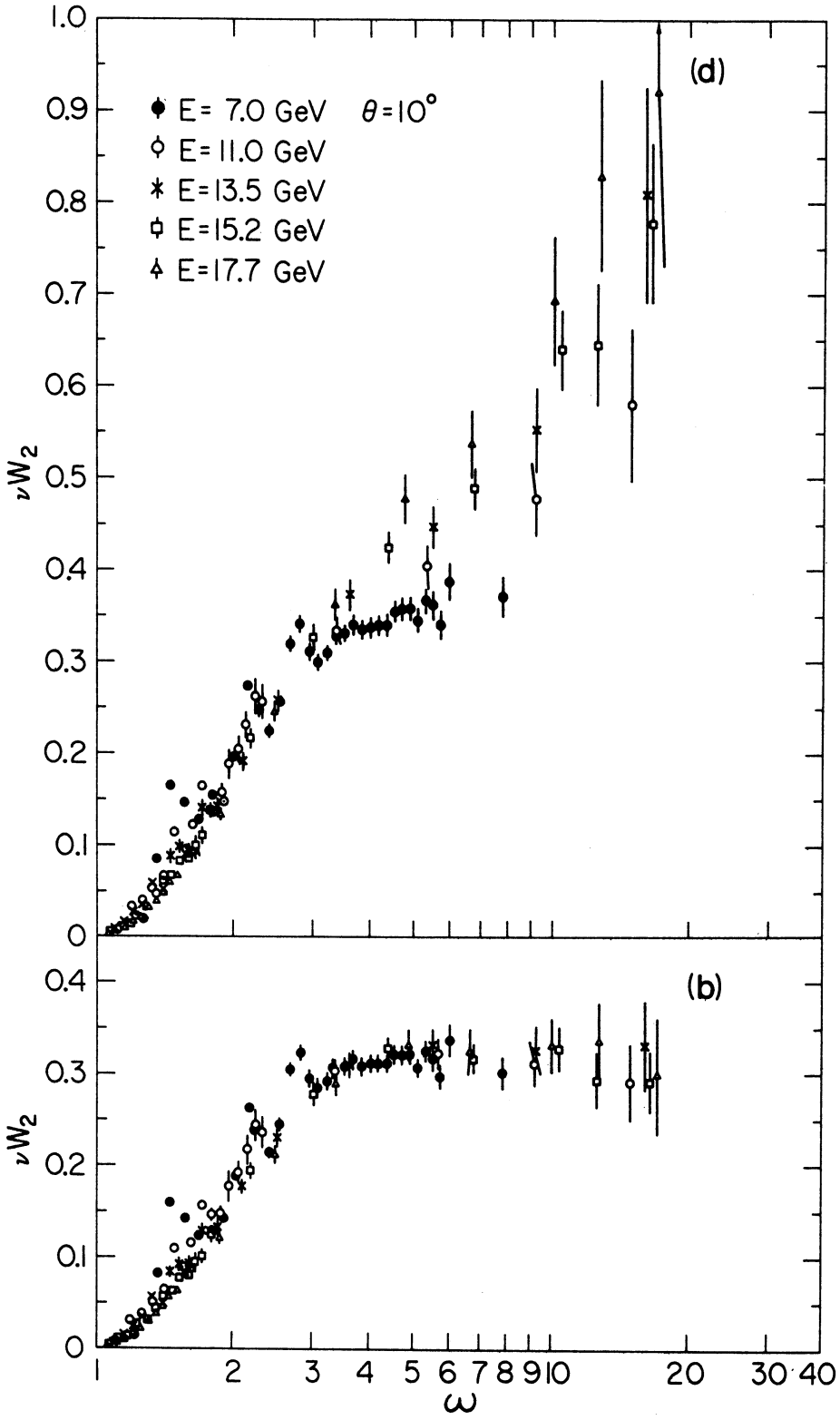

Fig. 22 Plot of $\nu W_2(\nu,q^2)$ versus $\omega = 2M\nu/q^2$ at $q^2 \geq 0.5$ GeV^2.
(a): $R = \infty$, (b): $R = 0$.

model, applied to the elastic form factors

$$G_{E(M)}(q^2) = \sum_{V=\rho,\omega,\varphi} (1 - q^2/m_V^2)^{-1} C^V_{E(M)} \qquad (5.23)$$

$$C^V_{E(M)} = g_{\gamma V}\, g^{E(M)}_{VNN},$$

is inconsistent with experiment at high values of q^2. For the isovector form factors

$$G^{V_3}_{E(M)}(q^2) = \frac{1}{2}(G^{\rho}_{E(M)} - G^{N}_{E(M)}) = (1 - \frac{q^2}{m_\rho^2})^{-1} C^{\rho}_{E(M)} \qquad (5.24)$$

to decrease like q^{-4} it is necessary either to include into the sum (5.23), at least one more (yet undiscovered) isovector meson (ρ' - meson) or to ascribe the additional q^2-dependence into vertex $g_{\gamma V}(q^2)$ and / or $g_{VNN}(q^2)$.

The fast decreasing of form factors finds more transparent and spectacular explanation within the framework of composite models.[41]

For the illustrative purposes we resort to simple example of the two-particle bound state of structureless constituents. In the non-relativistic approximation the e.m. form factor takes the familiar form

$$F(\vec{q}^2) = \int d^3r\, e^{i\vec{q}\cdot\vec{r}}\, \rho(r) = \int d^3r\, e^{i\vec{q}\cdot\vec{r}}\, |\Psi(r)|^2 =$$

$$= \frac{4\pi}{q} \int_0^\infty dr\, g(r) \sin qr, \qquad (5.25)$$

$$g(r) = r\,\Psi^2(r).$$

In the limit of $q^2 \to \infty$ the dominant contribution in Eq. (5.25) gives the small values of $r \to 0$:

$$F(\vec{q}^{\,2}) \underset{q^2 \to \infty}{\to} \frac{g(0)}{q^2} - \frac{g''(0)}{q^4} + \frac{g^{(IV)}(0)}{q^6} - \cdots , \qquad (5.26)$$

with $$g^{(n)}(0) = \frac{d^n g}{dr^n}\Big|_{r=0}$$

According to Eq.(5.26) it is possible to relate the rapid decreasing of the form factors to behaviour of the bound state wave function, hence, the interaction potential, at $r \to 0$.

For instance, the conditions

$$\begin{aligned} r\Psi^2(r) &\to 0 , \\ \Psi(r) &\to \text{const} , \end{aligned} \qquad (5.27)$$

are satisfied, if the Yukawa potential enters the Schroedinger equation.

Non-singular behaviour of the wave function at $r \to 0$ leads to small probability for particles in the bound state to have large momenta. Thus, our model consideration states an important relation between the absence of the high component in the momentum distribution of particles in the bound state and the rapid decreasing of the composite system e.m. form factors.

The relativistic consideration of the same problem on the basis of the two-particle Bethe-Salpeter equation does not change the qualitative behaviour of composite system

form factors, if the interaction between particles is such that in the non-relativistic limit it is reduced to the Yukawa potential.

5.3.2. Electroproduction of nucleon resonances.

The composite models can be applied also to the description of the nucleon resonance excitation. The resonance is assumed to be the (quasi) bound state of other "more simple" hadrons (like the pion and nucleon or pion and Δ-resonance) or the three-quark system.

For the constituents are allowed to have their own structure, one can try to define the transition form factors in terms of the elastic form factors of the constituents. The meaning of the approximations often made is readily explained in Fig.24.

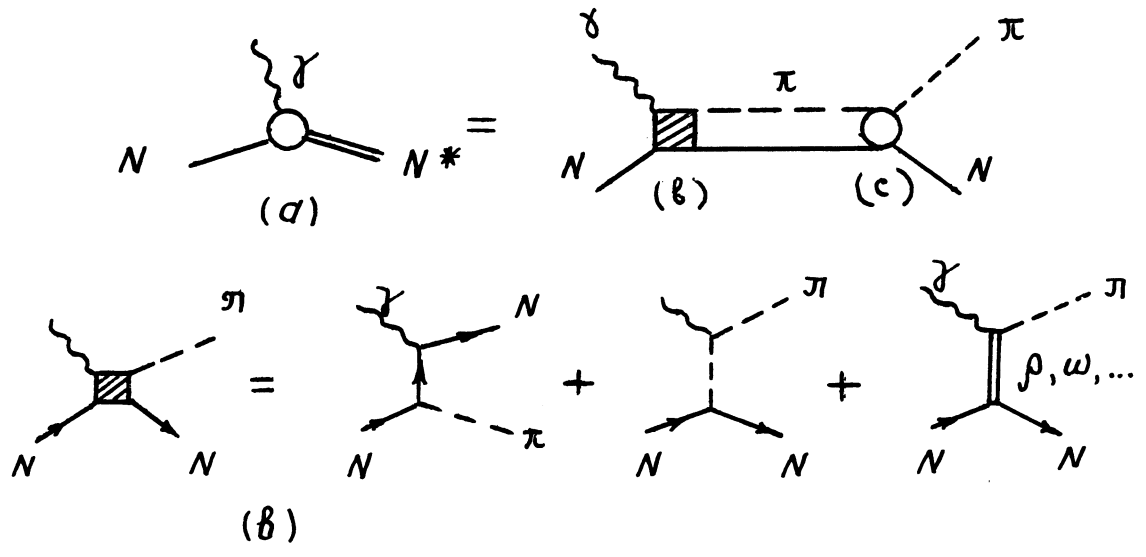

Fig. 23 Separation of the resonance electroexcitation into a transition potential (b), and the resonant final state interaction (c).

The transition potential (Fig. 21(b)) is defined by simple pole diagrams. The form factors of the constituents will enter just into the transition potential. The problem of resonant final state interaction is described by some universal function of $f = f(W)$, to be the same for all multipole transitions.[40)]

The total amplitude is then represented in the factorized form

$$M(W, q^2) = M_B(W, q^2)\ f(W) \qquad (5.28)$$

where $M_B(W, q^2)$ is the corresponding term in the multipole expansion of the full Born term contribution.

The threshold behaviour of the multipole amplitudes

$$\begin{aligned} &\text{El - transition :} && M_{El} \sim Q_i^{l-1} \\ &\text{Ml - transition :} && M_{Ml} \sim Q_i^{l} \\ &\text{Sl - transition :} && M_{Sl} \sim Q_i^{l} \end{aligned} \qquad (5.29)$$

where Q_i is the three momentum transfer in the rest frame of initial proton or final nucleon resonance, results in the enhancement of the higher spin resonance excitation as compared with the elastic scattering (see Fig. 20). In Eqs. (5.29) l is the multipolarity of the transitions in question. In fact, the case of elastic scattering provides a particular example of the general formula (5.29) for small $Q_i \equiv |\vec{q}|$:

$$\begin{aligned} |M_{S0}^{el}|^2 &= |\text{scalar monopole}|^2 \simeq G_E^2(q^2) \simeq Q_i^0 \simeq const \\ |M_{M1}^{el}|^2 &= |\text{magnetic dipole}|^2 \simeq q^2 G_M^2(q^2) \simeq Q_i^2 \end{aligned} \qquad (5.30)$$

To conclude, the Born term model describes the general behaviour of the transition form factors fairly well, although

further impovements in treating the final state interaction as well as more data concerning the pion form factor are certainly necessary.

5.3.3 Excitation of continuum in the deep-inelastic region.

Several different models were proposed for description of the inelastic ep - scattering with large energy and momentum transfers.

We start with the discussion of the "parton" model e.g. the model of the point - like constituents of nucleons.[42]

The large magnitude and rather weak q^2 - dependence of the inelastic interaction cross sections could be explained if proton was composed from the point - like constituents. We know neither the number (is it finite or infinite?), nor the properties of partons (charge, mass, spin) and their internal motion dynamics. Concerning what follows, it is, however, very important to assume that the average parton momenta do not take too large values. Then, in the limit of an infinite - large momentum of an incident electron, it seems natural to apply the usual impulse approximation, having represented the e-p interaction amplitude as a sum of the interaction amplitudes of an electron with "free" or "long-lived" partons, each of them having the momentum

$$p_\mu^i = x_i P_\mu \qquad (5.3I)$$

where $x_i < I$, P_μ is the nucleon momentum in the c.m.s. (see Fig. 24)

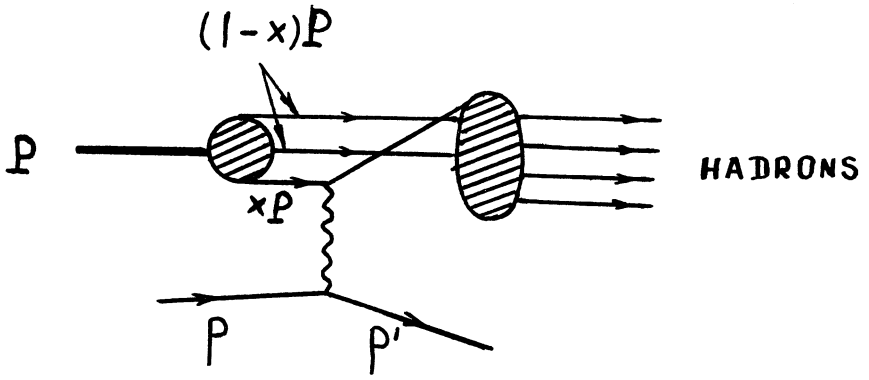

Fig. 24 Kinematics of ineslastic electron scattering in the parton model.

The large values of the energy and momentum transfer make it reasonable to consider the interaction time of electron with nucleon to be much less than the characteristic time needed for partons to change markedly their momenta due to internal motion. Furthermore, at large transferred momentum one can neglect the correlation between the coordinates and momenta of various partons during the process of the electron-nucleon interaction and write the structure function $W_2(\nu, q^2)$ in the form

$$e^2 W_2(\nu, q^2) = \sum_N P(N) \sum_{i=1}^{N} e_i^2 \int_0^1 dx\, f_N(x)\, W_2^{(i)}(\nu, q^2, x), \qquad (5.32)$$

$$\sum_N P(N) = 1, \qquad (5.33)$$

$$\int_0^1 f(x)\, dx = 1. \qquad (5.34)$$

where $P(N)$ is the probability of N partons occurring, $e_i = Q_i \cdot e$ is the i'th parton charge, $f_N(x)$ gives the distribution of longitudinal momenta of the partons, while $W_2^{(i)}$

gives the contribution of a single parton to $W_2(\nu, q^2)$.

During the scattering the point - like parton is keeping its mass and charge, which enables us to write

$$\frac{p_\mu p_\nu}{M^2} W_2(\nu, q^2) = \sum_N \sum_i \int dx\, P(N) f_N(x) \frac{p_\mu^{(i)} p_\nu^{(i)}}{p_0^{(i)}} Q_i^2 \delta\left(p^{(i)} q + \frac{q^2}{2}\right) \qquad (5.35)$$

Making use of Eq.(5.3I), one gets

$$\nu W_2(\nu, q^2) = \sum_N P(N) \left(\sum_{i=1}^{N} Q_i^2\right) \times f_N(x) \Big|_{x = -\frac{q^2}{2M\nu}} \qquad (5.36)$$

Hence, the structure function $\nu W_2(\nu, q^2)$ has the form

$$\nu W_2(\nu, q^2) = F\left(-\frac{q^2}{2M\nu}\right) \equiv F\left(-\frac{q^2}{2pq}\right) \qquad (5.37)$$

which is invariant under the scale transformation

$$q \to \lambda q\,, \qquad P \to \lambda P \qquad (5.38)$$

and is described by the universal function of one variable.

This very important conclusion gives evidence for the absence of any "internal" parameter with dimension of mass in the region of deep - inelastic lepton-hadron interaction. Unlike $W_2(\nu, q^2)$, the explicit form of $W_1(\nu, q^2)$ depends on the parton spin.

It is not difficult to show, that

$$W_1(\nu, q^2) = \begin{cases} -\frac{\nu^2}{q^2} W_2(\nu, q^2) & \text{for } s = \frac{1}{2} \qquad (5.39) \\ 0 & \text{for } s = 0 \qquad (5.40) \end{cases}$$

From comparison of Eqs.(5.39) and (5.40) with (5.II) we find at $\nu^2 \gg |q^2|$

$$R = \frac{\sigma_\ell}{\sigma_t} = \begin{cases} 0 & \text{for } s = \frac{1}{2} \quad (5.4I) \\ \infty & \text{for } s = 0 \quad (5.42) \end{cases}$$

The data favours (5.4I) which means that the partons should be the fermions.

Within the parton model a number of interesting sum rules were obtained.

By the normalization (5.34) we get

$$\int_0^\infty d\nu\, W_2(\nu, q^2) = \int_0^\infty dx\, \frac{F(x)}{x} = \sum_N P(N) \sum_{i=1}^N Q_i^2 \,. \qquad (5.43)$$

Assuming the symmetric distribution of longitudinal momenta among the partons

$$\int_0^1 x f_N(x)\, dx = \frac{1}{N} \,, \qquad (5.44)$$

and making use of Eq.(5.36) one obtains

$$-\frac{q^2}{2M} \int_0^\infty \frac{d\nu}{\nu} W_2(\nu, q^2) = \int_0^1 dx\, F(x) = \sum_N P(N) \frac{1}{N} \sum_{i=1}^N Q_i^2 = \overline{Q_i^2} \,. \qquad (5.45)$$

Numerically, the calculation of integrals in (5.44) and (5.45) gives

$$\int_{0.05}^1 \frac{F(x)}{x}\, dx = 0.7 \qquad (5.46a)$$

$$\int_{0.05}^1 F(x)\, dx = 0.18 \qquad (5.46b)$$

Let us assume now that the partons are quarks. If the proton is composed of three quarks, we would have

$$\sum_{i=1}^{3} Q_i^2 = \frac{4}{9} + \frac{4}{9} + \frac{1}{9} = 1 \qquad (5.47a)$$

$$\overline{Q_i^2} = \frac{1}{3} \sum_{i=1}^{3} Q_i^2 = \frac{1}{3} \qquad (5.47b)$$

The magnitude of (5.47b) is too big to fit the data.

Another extreme case is an infinite sea of quark-anti-quark pairs with average charge squared equal to

$$\overline{Q_i^2} = \frac{1}{3}\left(\frac{1}{9} + \frac{1}{9} + \frac{4}{9}\right) = \frac{2}{9} \simeq 0{,}22 \qquad (5.48)$$

which is reasonably close to Eq.(5.46b).

If the present trend of the data will persist, then the integral (5.43) will diverge logarithmically e.g.

$$W_2(\nu, q^2) \sim \frac{q^2 \sigma_t(\nu, q^2)}{\nu} \sim \frac{const}{\nu} \qquad (5.49)$$

Eq.(5.49) is in accordance with the usual diffraction model, where the Pomeranchuk pole gives asymptotically

$$\sigma_t(\nu, q^2) \xrightarrow[\nu \to \infty]{} \beta(q^2)\, \nu^{\alpha_P(0)-1} = \beta(q^2) \qquad (5.50)$$

To retain the scale invariance condition (5.37) we should put

$$\beta_P(q^2) \sim \frac{1}{q^2} \qquad (5.5I)$$

in which case

$$\nu W_2(\nu, q^2) \longrightarrow const \qquad (5.52)$$

in the Bjorken limit of $\nu \gg M$, $|q^2| \gg M^2$, $2M\nu/q^2$ = fixed.

In the non-asymptotic energy region the pure hadronic cross sections get significant contributions from the lower

Regge - trajectories with $\alpha < I$ (the P', ρ, A_2 - trajectories).

What is their role in the total electroproduction cross sections?

At this point we shall make contact with presently popular duality hypothesis.

In particular, we shall assume, that

a) in the sense of the finite energy sum rules the t-channel contributions of "usual" Regge - trajectories (ρ', ρ, A_2 etc.) are built from the nucleon resonance contributions in the S - channel.

b) the Pomeranchon is built from the non-resonance background in the S - channel.

As we have seen in the precedent section, the nucleon resonance excitation decreases rapidly with increasing q^2. The point (a) just adopted leads to a similar fast decreasing of the residue functions $\beta_i(q^2)$ of "usual" Regge - trajectories at large q^2.

The non-resonance continuum excitation decreases much slower, approximately like q^{-2}. Hence, the q^2 - dependence of $\beta_P(q^2)$ should be the same (see formula (5.5I)).

These considerations form the base for a number of interesting predictions [43]:

I. At large q^2 the absorption cross section of virtual photons by hadrons should be pure diffraction one even at relatively moderate energies. The deviations from constant cross section should decrease rapidly with q^2.

The ratio $R = \sigma_l/\sigma_t$ should also be constant.

2. The difference between $\sigma_{\gamma p}(\nu, q^2)$ and $\sigma_{\gamma n}(\nu, q^2)$ is defined presumably by the A_2 - trajectory contribution. Hence, it should decrease rapidly with increasing q^2.

3. The q^2 - dependence of the amplitude for specific inelastic channels should be different for diffraction and non-diffraction processes. For example, the cross section $\frac{d\sigma}{dt}(ep \to e\rho^0 p)$, which includes the Pomeranchon contribution should display much more weak q^2-dependence in comparison, say, with $\frac{d\sigma}{dt}(ep \to e\pi^+ n)$, which should, likely, vary with q^2 similar to the nucleon form factors.

All these predictions can be tested directly by the corresponding experiments.

In summary, the elastic and inelastic electron-nucleon scattering will serve as the extremely valuable source of information on the internal structure of hadrons, on the properties of e.m. current operator and dynamics of photon-hadron interactions. Especially important and interesting features, discovered recently, are the scale invariance of the lepton-hadron interactions at deep inelastic region, and the evidence for dynamical dominance at $q^2 \gg M^2$, $\nu^2 \gg M^2$ of the current structure, built from the fermion fields.

6. ANNIHILATION OF LEPTON PAIRS INTO HADRONS AND PAIR PRODUCTION IN HADRON REACTIONS.

6.I Kinematics and definition of the spectral function $\rho(q^2)$.

The elastic and inelastic hadron form factors may be studied in the time-like region of $q^2 > 0$ via the pair annihilation processes

$$e^+ + e^- \longrightarrow \text{hadrons} \qquad (6.I)$$

or in the lepton pair production reactions

$$(\gamma, \pi, N, \ldots) + A \longrightarrow e^+ + e^- + \text{hadrons} \qquad (6.2)$$

We consider first the annihilation reactions, which are intensively explored presently in the colliding $e^+ - e^-$ beam experiments.

In the one-photon approximation the matrix element of reaction (6.I) takes the form

$$T(e^+e^- \to \text{hadrons}) = \frac{4\pi\alpha}{q^2} \langle p_n | J_\mu(0) | 0 \rangle \langle 0 | j_\mu(0) | p_+, p_- \rangle, \qquad (6.3)$$

$$q = p_+ + p_- = p_n,$$

where p_+ and p_- are the leptonic momenta, p_n is the final hadronic state momentum.

As in the precedent section we define the tensor W

$$W_{\mu\nu} = (2\pi)^3 \sum \langle 0 | J_\mu(0) | p_n \rangle \langle p_n | J_\nu(0) | 0 \rangle \delta^{(4)}(q - p_n) =$$
$$= -\left(g_{\mu\nu} - \frac{q_\mu q_\nu}{q^2}\right) \rho(q^2) \qquad (6.4)$$

which is gauge-invariant and contains all the dynamics concerning the conversion of virtual photon into hadrons. Eq.(6.4) defines the spectral function $\rho(q^2)$ which is the very impor-

tant quantity of the theory of e.m. interactions. Being connected with the vacuum polarization (see Fig. 25a) by the strong interactions, it enters many expressions for the physically interesting quantities, like, say, the anomalous magnetic moment of leptons (Fig. 25b), the Feynman diagrams for the lepton scattering (Fig. 25c) etc.

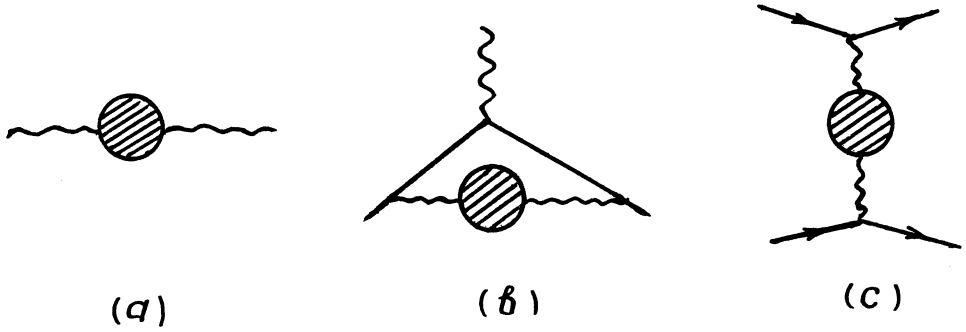

Fig. 25 Feynman graphs of the vacuum polarization.

Furthermore, the integral

$$C = \int \frac{\rho(q^2)}{q^2}\, dq^2 \qquad (6.5)$$

is related to the equal-time commutator

$$\delta(x_0 - x_0')\left\langle \left[J_0^{e.m.}(x), J_k^{e.m.}(x') \right] \right\rangle_{\substack{\text{vacuum} \\ k=1,2,3}} = -i C \partial_k \delta^{(4)}(x - x'), \qquad (6.6)$$

which plays the central role in the current algebra theory.

The definitions (6.5) and (6.6) state the close connection between the current algebra models and asymptotic behaviour of $\rho(q^2)$ at $q^2 \to \infty$.

Therefore, it is a very important and advantageous circumstance that $\rho(q^2)$ can be measured directly, since it enters the total cross section of lepton annihilation into

hadrons

$$\sigma_{tot}(e^+e^- \to \text{hadrons}) = \frac{16\pi^3\alpha^2}{q^4}\rho(q^2) \qquad (6.7)$$

6.2 Scale invariance hypothesis and asymptotic behaviour of $\rho(q^2)$.

The conjecture on the scale invariance of the tensor (6.4) results in an interesting conclusion concerning the asymptotic behaviour of $\rho(q^2)$ [44].

In the system of units in which the dimensionalities of mass, energy, momentum and the inverse of length are the same, we have for the current dimensionality

$$[J_\mu] = m^3 \qquad (6.8)$$

Using Eq.(6.8), it is not difficult to find:

$$[W_{\mu\nu}] = m^2 \qquad (6.9)$$

Hence, under the scale transformation $q \to \lambda q$, $W_{\mu\nu}$ behaves as follows:

$$W_{\mu\nu}(\lambda q) = \lambda^2 W_{\mu\nu}(q) \qquad (6.10)$$

and we get finally in the asymptotic region of $q \to \infty$:

$$\rho(q^2) \Longrightarrow \text{const} \cdot q^2 , \qquad (6.11)$$

$$\sigma_{tot}(e^+e^- \to \text{hadrons}) \sim \frac{const}{q^2} \sim \frac{const}{E^2} , \qquad (6.12)$$

where $E = E_+ + E_-$ is the energy of colliding leptons in the c.m.s.

According to Eq.(6.11) the constant C in (6.6) diverges linearly. Just such a kind of divergence was found to occur if the equal-time commutator is calculated with the help of the quark model [45], where the e.m. current is of the form

$$J_\mu(x) = e\,\bar{q}(x)\,\gamma_\mu\,Q\,q(x)$$

$$q = \begin{pmatrix} p \\ n \\ \lambda \end{pmatrix}, \quad Q = \frac{1}{3}\begin{pmatrix} 2 & 0 & 0 \\ 0 & -1 & 0 \\ 0 & 0 & -1 \end{pmatrix} \qquad (6.13)$$

with p, n, λ denoting the members of the quark triplet.

6.3 Asymptotic SU(3) - symmetry and the spectral sum rule.

Using the SU(3) - properties of the hadron e.m. current fixed by Eq.(3.6), we can write for $\rho(q^2)$

$$\rho(q^2) = \rho^{33}(q^2) + \frac{1}{3}\rho^{88}(q^2) \qquad (6.14)$$

Now we make the assumption that the SU(3) symmetry becomes exact in the asymptotic region $q \to \infty$, so that the constants C^3 and C^8, defined analogously C in Eq.(6.6), are equal to each other

$$C^3 - C^8 = 0 \qquad (6.15a)$$

which means

$$\int_0^\infty \frac{\rho^{33}(q^2) - \rho^{88}(q^2)}{q^2}\,dq^2 = 0 \,. \qquad (6.15b)$$

Eq.(6.15b) may be written also as

$$\frac{1}{3}\int_{4m_\pi^2}^{\infty} s\sigma(e^+e^- \to I=1)\,ds = \int_{9m_\pi^2}^{\infty} s\sigma(e^+e^- \to I=0)\,ds \qquad (6.16)$$

where $\sigma(e^+e- \to I = 0,1)$ are the annihilation cross sections into hadronic states with fixed values of the isospin I. At $s = q^2 = m_V^2$ $(V = \rho, \omega, \varphi)$ the cross section $\sigma(s)$ has the resonance behaviour, approximated usually by the

Breit-Wigner formula

$$\sigma(s) = \frac{12\pi}{s} \cdot \frac{m_v^2 \Gamma(v \to e^+e^-)\Gamma_{tot}(v)}{(s-m_v^2)^2 + m_v^2 \Gamma_{tot}^2(v)} \cdot \qquad (6.17)$$

After substitution of Eq.(6.17) into (6.16) and evaluation of the corresponding integrals in the narrow width approximation, we get the well-known sum rule for the leptonic widths of ρ^0, ω, φ -mesons[46)]

$$\frac{1}{3} m_\rho \Gamma_\rho - m_\omega \Gamma_\omega - m_\varphi \Gamma_\varphi = 0 \qquad (6.18)$$

where

$$\Gamma_v \equiv \Gamma(v \to e^+e^-) = \frac{1}{3} g_{\gamma v}^2 \alpha m_v + O\left(\frac{m_e^4}{m_v^4}\right) \qquad (6.19)$$

Note, that in the current literature other definitions of the photon-vector-meson coupling constant are also used

$$g_{\gamma v} \equiv \frac{\sqrt{4\pi\alpha}}{g_v} \equiv \frac{\sqrt{4\pi\alpha}}{f_v} \equiv \frac{\sqrt{4\pi\alpha}}{2\gamma_v} \qquad (6.20)$$

6.4 Experimental widths of ρ, ω, φ mesons from the colliding beams data.

The study of the resonance characteristics (like the form of the excitation curve and the values of the cross section in the maximum) of the reactions

$$e^+e^- \to \rho^0 \to \pi^+\pi^-$$
$$e^+e^- \to \omega \to \pi^+\pi^-\pi^0$$
$$e^+e^- \to \varphi \to \begin{cases} K^+K^- \\ K^0\bar{K}^0 \\ \pi^+\pi^-\pi^0 \end{cases}$$

provides an important information on the mass and widths of the neutral vector mesons. Table 8 shows the data concerning the ρ^0, ω, φ widths, obtained from the storage rings experiments.[47]

T a b l e 8

Experimental values of the ρ^0, ω, φ widths.

V	ρ	ω	φ
$\Gamma(V \to e^+e^-)$ kev	7.4 ± 0.5	0.94 ± 0.18	1.58 ± 0.13
$g_V^2/4\pi$	$1,99 \pm 0,11$	14.9 ± 2.8	11.5 ± 0.9
$\Gamma_{tot}(V)$ Mev	120 ± 4	12.2 ± 1.3	4.24 ± 0.28

Inserting the masses and the leptonic widths of V^0 - mesons into the sum rule (6.18), one finds

$$\Sigma = \frac{1}{3} m_\rho \Gamma_\rho - m_\omega \Gamma_\omega - m_\varphi \Gamma_\varphi = -0,44 \pm 0,24 \ \text{Mev}^2 \qquad (6.21)$$

which satisfactorily agrees with Eq.(6.18).

The contribution of the neutral vector mesons in the muon anomalous magnetic moment according to the Feynman diagram in Fig. 25(b) was found to be [9]

$$(\Delta a_\mu)_{\rho,\omega,\varphi} = (6,5 \pm 0,5) \times 10^{-8} = (5.0 \pm 0.4) \frac{\alpha^3}{\pi^3} \qquad (6.22)$$

Numerically, the value (6.22) is 5 times less than the experimental errors in measurement of a_μ

6.5 Rho dominance and the pion form factor.

With the definition of the pion form factor in the time-like region of $q^2 > 0$

$$\langle 0 | J_\mu(0) | \pi(K_+), \pi(K_-) \rangle = (2\pi)^{-3} (4K_+^0 K_-^0)^{-1/2} (K_+ - K_-)_\mu F_\pi(q^2) \qquad (6.23)$$

one can obtain the formula for the lepton pair annihilation cross section into two charged pions

$$\sigma(e^+e^-\to\pi^+\pi^-) = \frac{\pi\alpha^2}{3q^2}\beta^3 \left|F_\pi(q^2)\right|^2$$
$$\beta = \frac{|\vec{K}|}{K^0} = \left(\frac{q^2-4m_\pi^2}{q^2}\right)^{1/2}, \quad q = K_+ + K_- = 2K . \tag{6.24}$$

Having introduced the coupling constant $g_{\rho\pi\pi}$, that defines the width of decay $\rho\to 2\pi$

$$\Gamma(\rho\to 2\pi) \simeq \Gamma_{tot}(\rho) = \frac{g^2_{\rho\pi\pi}}{4\pi}\cdot\frac{m_\rho}{12}\cdot\left(\frac{m_\rho^2-4m_\pi^2}{m_\rho^2}\right)^{3/2} \tag{6.25}$$

we note from a comparison of Eqs.(6.I7) and (6.24)

$$\left|F_\pi(q^2)\right|^2 = \left(\frac{g_{\rho\pi\pi}}{g_\rho}\right)^2 \cdot \frac{m_\rho^4}{(q^2-m_\rho^2)^2 + m_\rho^2\Gamma^2_{tot}(\rho)} \tag{6.26}$$

The form factor $F_\pi(q^2)$ should meet the normalization condition

$$F_\pi(0) = I . \tag{6.27}$$

In the zero - width approximation ($\Gamma_{tot}(\rho)\to 0$) we would have as a consistency condition of Eqs.(6.26) and (6.27)

$$g_{\rho\pi\pi} = g_\rho . \tag{6.28}$$

The last equality is in striking agreement with experiment

$$\left(\frac{g^2_{\rho\pi\pi}}{4\pi}\right)_{exp} = 2.1\pm 0.2 \simeq \left(\frac{g^2_\rho}{4\pi}\right)_{exp} = 1.99\pm 0.11 \tag{6.29}$$

The rho-meson dominance for the pion form factor

$$F_\pi(q^2) = \frac{m_\rho^2}{m^2-q^2} \tag{6.30}$$

implies the following value for e.m. radius

$$\left(<r^2>_\pi\right)^{1/2} = \left(-6\,F_\pi'(0)\right)^{1/2} = \frac{\sqrt{6}}{m_\rho} \simeq 0{,}6\,fm\,, \qquad (6.31)$$

which is less than the nucleon isovector radii

$$\left(<r_{ch}^2>^V\right)^{1/2} = \left(-6\,G_E^{V\prime}(0)\right)^{1/2} \simeq 0{,}82\,fm$$

$$\left(<r_1^2>^V\right)^{1/2} = \left(-6\,F_1^{V\prime}(0)\right)^{1/2} = 0{,}74\,fm \qquad (6.32)$$

and also somewhat less than the magnitude

$$\left(<r_\pi^2>\right)^{1/2} = (0{,}8 \pm 0{,}1)\,fm \qquad (6.33)$$

obtained from an analysis of the reaction $ep \to e\pi^+ n$ at small energies[48].

The explicit form of the finite width corrections to Eq.(6.30) depends on the model assumptions about the π-π phase - shift energy dependence as well as some additional assumptions concerning the analytic properties of the form factor (such as the absense of zeros etc.)

Of great help there would be a direct measurement of the pion radius in a process of the pion scattering from the atomic electrons in the multi - GeV region. The high energy pion beam is necessary since the maximum invariant square of the momentum transfer to the target electron is

$$t_{max} \simeq \frac{2 m_e E_L(\pi)}{1 + m_\pi^2 / 2 m_e E_L(\pi)} = \begin{cases} (190\ \text{MeV})^2 \text{ for } E_L = 50\ \text{GeV} \\ (630\ \text{MeV})^2 \text{ for } E_L = 400\ \text{GeV} \end{cases}$$

6.6 Problem of the ω-φ mixing and the storage rings data.

It is of considerable interest to compare the experimental values of g_v's with the broken SU(3) symmetry predictions.

The classic Gell-Mann-Okubo mass relation is well known to define the mass m_8 of the isoscalar member entering the vector meson octet

$$m_8 = \left[\frac{1}{3} (4 m_{K^*}^2 - m_\rho^2 \right]^{1/2} = 928 \text{ MeV} \qquad (6.34)$$

which equals neither m_ω = 782 MeV, nor m_φ = 1020 MeV.

The hypothesis was put forward about the mixing of the unitary singlet state ω_1 and the octet state ω_8 due to the SU(3) symmetry breaking.

One can introduce the symmetry breaking terms in the initial SU(3) symmetric Lagrangian of vector meson field

$$\mathcal{L}_{sym} = -\frac{1}{4} F^a_{\mu\nu} F_a^{\mu\nu} - \frac{1}{2} m_0^2 V^a_\mu V_a^\mu \qquad (6.35)$$

$$a = 1, 2, \ldots 8$$

in two different ways : either into the "mass term" (the second term in Eq.(6.35)) or into the "kinetic term" (the first term in (6.35)).

In the first case we have the mass formula

$$\frac{1}{3} (4 m_{K^*}^2 - m_\rho^2) = m_\varphi^2 \cos\theta + m_\omega^2 \sin^2\theta \qquad (6.36)$$

with the mixing angle $\theta = 40^\circ$, while in the second case one can obtain the Coleman-Schnitzer mass formula[49]

$$\frac{1}{3} \left(\frac{4}{m_{K^*}^2} - \frac{1}{m_\rho^2} \right) = \frac{\cos^2\theta_{inv}}{m_\varphi^2} + \frac{\sin^2\theta_{inv}}{m_\omega^2} \qquad (6.37)$$

with $\theta_{inv} = 28{,}6.^{o}$

There is a beautiful possibility to formulate the singlet-octet mixing conjecture within the framework of the vector meson dominance model and current - field identity of Eq. (4.5) [50].

Evidently, with using Eq.(4.5) we can write

$$J^{s}_{e.m}(x) = \frac{m_\varphi^2}{g_\varphi}\Phi_\mu(x) + \frac{m_\omega^2}{g_\omega}\omega_\mu(x) \equiv \frac{1}{2}Y_\mu(x) = \\ = \frac{1}{2g_Y}\left(m_\varphi^2 \cos\theta_Y \Phi_\mu(x) - m_\omega^2 \sin\theta_Y \omega_\mu(x)\right) \tag{6.38}$$

where Y_μ is the hypercharge current, g_Y is the universal coupling constant of vector mesons with the hypercharge current, θ_Y is the corresponding mixing angle, introduced without any reference to a particular model of the SU(3) breaking.

For the baryon current $B_\mu(x)$ we have

$$B_\mu(x) = \frac{1}{g_B}\left(m_\varphi^2 \sin\theta_B \Phi_\mu(x) + m_\omega^2 \cos\theta_B \omega_\mu(x)\right) \tag{6.39}$$

In general, the mixing angles θ_Y and θ_B are different. We consider below two particular models of the SU(3) breaking:

a) the "mass mixing" model, which is specified by the equality $\theta_Y = \theta_B = \theta$ and by the mass formula of Eq.(6.36)

b) the "current mixing" model, specified by the relation

$$\tan\theta_{inv} = \frac{m_\varphi}{m_\omega}\tan\theta_B = \frac{m_\omega}{m_\varphi}\tan\theta_Y \tag{6.40}$$

and by the mass formula of Eq.(6.37).

It follows from the definition (6.38) and Eqs.(6.I9), (6.20) that

$$\frac{\Gamma(\omega \to e^+e^-)}{\Gamma(\varphi \to e^+e^-)} = \frac{m_\omega}{m_\varphi} \tan^2 \theta_Y \qquad (6.4I)$$

With the help of the data, listed in Table 8, we find

$$|\theta_Y| = 41{,}6^\circ \pm 3{,}0^\circ. \qquad (6.42)$$

The magnitude of the "intermediate" angle θ

$$\tan^2 \theta = \tan \theta_Y \cdot \tan \theta_B \qquad (6.43)$$

can be obtained in a model-independent manner from the reaction $e^+e^- \to \varphi \to K^+K^-$.

Indeed, using Eqs.(6.I7), (6.I9), (6.20) and (6.25) with evident replacement $\rho \to \varphi$, $\pi \to K$, where needed, we get

$$\sigma_{e^+e^- \to K^+K^-}(s = m_\varphi^2) = \frac{\pi\alpha^2}{3\Gamma_{tot}^2(\varphi)} \left(1 - \frac{4m_K^2}{m_\varphi^2}\right)^{3/2} \cdot \frac{g_{\varphi KK}^2}{g_\varphi^2} \qquad (6.45)$$

We recall the definition

$$\frac{1}{g_\varphi} = \frac{\cos\theta_Y}{2g_Y} \qquad (6.46)$$

In accordance with the main dynamical assumption of VMD on the smoothness of the vector current form factors, we put

$$g_{\varphi KK}(m_\varphi^2) = g_{\varphi KK}(0) = m_\varphi^2 \langle K^+(\vec{p}=0)|\Phi_\mu(0)|K^+(\vec{p}=0)\rangle =$$

$$= \frac{1}{\cos(\theta_Y - \theta_B)} \left[g_Y \cos\theta_B \langle K^+|Y_\mu(0)|K^+\rangle + g_B \sin\theta_Y \langle K^+|B_\mu(0)K^+\rangle \right]$$

$$= \frac{g_Y \cos\theta_B}{\cos(\theta_Y - \theta_B)} \qquad (6.47)$$

In Eq.(6.47) we have used Eqs.(6.38), (6.39) to define in terms of $Y_\mu(x)$ and $B_\mu(x)$, and the normalization of the hypercharge and baryon currents

$$\begin{aligned} &\langle K^+(\vec{p}=0)|\, Y_\mu(0)\,|K^+(\vec{p}=0)\rangle = 1\,, \\ &\langle K^+(\vec{p}=0)|\, B_\mu(0)\,|K^+(\vec{p}=0)\rangle = 0\,. \end{aligned} \tag{6.48}$$

At last, using Eqs.(6.47), (6.46) and (6.45) we find

$$\sigma_{e^+e^-\to K^+K^-}(s=m_\varphi^2) = \frac{\pi\alpha^2}{12}\cdot\frac{\cos^4\theta}{\Gamma_{tot}^2(\varphi)}\cdot\left[1-\frac{4m_K^2}{m_\varphi^2}\right]^{3/2} \tag{6.49}$$

Comparison of Eq.(6.49) with the data gives [47]

$$|\theta| = 31{,}5^\circ \tag{6.50}$$

which agrees better with the current - mixing model of Eqs. (6.40) and (6.37).

6.7 Photoproduction of lepton pairs from the hadron targets.

Consider the process

$$\gamma + A \to l^+ + l^- + A \tag{6.51}$$

where A represents either a nucleus or a nucleon. The diagrams which might contribute to the process (6.51) are shown in Fig. 26.

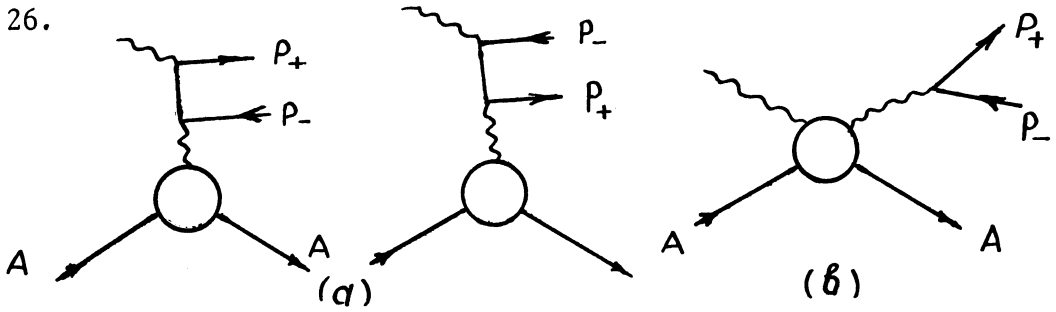

Fig. 26 (a) Diagrams for the Bethe-Heitler production of lepton pairs.

(b) Diagram of the "Compton" contribution.

In general, the cross section will include the interference between two types of Feynman diagrams

$$|M_{tot}|^2 = |M_{BH}|^2 + |M_C|^2 + 2\,Re\,(M^*_{BH} M_C) \qquad (6.52)$$

Since the pure quantum electrodynamic Bethe-Heitler matrix element M_{BH} has no imaginary part in the lowest order in α, the interference term in Eq.(6.52) measures the real part of the "Compton" matrix element M_C.

Therefore, the measurement of the difference

$$\Delta = d\sigma(\vec{p}_+, \vec{p}_-) - d\sigma(\vec{p}_+ \rightleftarrows \vec{p}_-) \sim 4\,Re\,(M^*_{BH} \cdot M_C) \qquad (6.53)$$

by observing asymmetrically photoproduced lepton pairs yields the value of $Re\,M_C$ or, equivalently, the phase difference between the Bethe-Heitler and "Compton" amplitudes.

With the definition of the phase angle difference Δ

$$M_{tot} = M_{BH} + M_C = M_{BH} + i\,\exp(i\Delta)\cdot|M_C| \qquad (6.54)$$

it was found [51], that Δ is consistent with the zero-value

$$\Delta = 15^0 \pm 25^0 \qquad (6.55)$$

which means, that the "Compton" amplitude in photoproduction of the electron-positron pairs from carbon is almost imaginary one at 5 GeV [51].

At the symmetric kinematics ($|\vec{p}_+| = |\vec{p}_-|$, $\theta_- = \theta_+$) the leptonic parts of diagrams (a) and (b) in Fig. 26 have the definite and opposite in sign charge parity. Hence, there is no interference between M_{BH} and M_C (the Furry's theorem).

In this case we can subtract the Bethe-Heitler contri-

bution (to be computed theoretically with high precision) from the total excitation curve to study further only the virtual Compton amplitude.

In the region of $(P_+ + P_-)^2 = m_V^2$, $(V = \rho, \omega)$, the Compton process (Fig. 26(b)) is dominated by the sum of two diagrams for the coherent ρ° and ω production with subsequent decay into lepton pairs

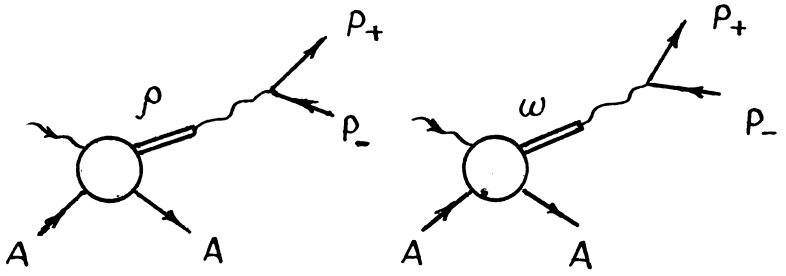

Fig. 27 Diagrams for coherent production of vector mesons with decay into lepton pairs.

It is clear, the shape of the mass spectrum of final pairs should display the ρ-ω interference pattern. This interference was observed recently in the experiments with high mass resolution (Δ m = ± 5 MeV). The reactions in question were

$$\text{DESY}^{22}: \quad \gamma\,(5.12\,\text{GeV}) + Be^9 \rightarrow e^+ + e^- + Be^9 \qquad (6.56a)$$

$$\text{Daresbury}^{52}: \quad \gamma\,(4.1\,\text{GeV}) + C^{12} \rightarrow e^+ + e^- + C^{12} \qquad (6.56b)$$

As an example, the experimentally measured lepton mass spectrum[22] is shown in Fig. 28. The peak at the place of ω-meson is clearly seen.

One cannot yet make definite conclusion on the relative

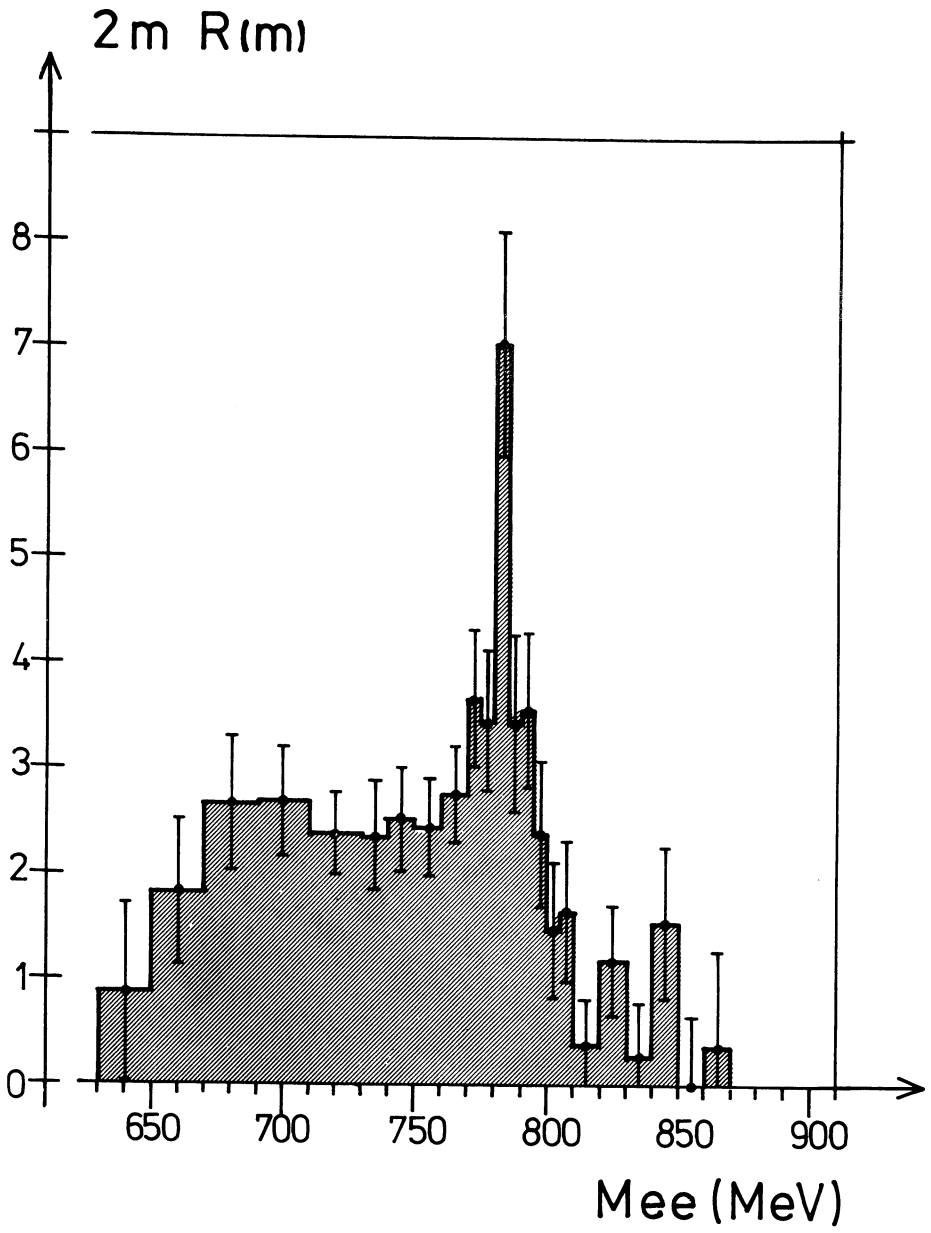

Fig. 28 Lepton pair mass distribution measured in the reaction $\gamma + Be^9 \rightarrow e^+ + e^- + Be^9$ at 5 GeV. (From Ref. 22).

phase of the ρ and ω production amplitudes, for various groups give different values for that quantity

$$\Delta_{\rho\omega}(\text{DESY}) = (22 \pm 25)\ \text{deg}\ , \tag{6.57a}$$

$$\Delta_{\rho\omega}(\text{Daresbury}) = (100\ ^{+38}_{-30})\ \text{deg}. \tag{6.57b}$$

6.8 Lepton pair production in hadron collisions.

The reactions of the type

$$(\pi\ ,\ K,\ N,\ldots) + A \rightarrow l^+ + l^- + \text{hadrons} \tag{6.58}$$

are of interest for many reasons.

In fact, in the process

$$\pi^- + p \rightarrow V^0 + n \rightarrow e^+ + e^- + n \tag{6.59}$$

first studies were made on the leptonic decays of the neutral vector mesons[53,54].

The reaction (6.59) may serve as a complementary tool, as compared to the pion electroproduction, for studying the hadron e.m. form factors in the time-like region of $q^2 > 0$.

The preliminary results were quite recently obtained[55] on the deep inelastic process

$$p\,(22 \div 30\ \text{GeV}) + U^{239} \rightarrow \mu^+ + \mu^- + \text{anything} \tag{6.60}$$

which was shown to decrease rapidly with invariant mass of μ-pairs. In the region $2\ \text{GeV} \leq m_{\mu^+\mu^-} \leq 6\ \text{GeV}$ the cross section of (6.60) falls by three orders of magnitude.

So, we have seen in this section, that the study of the lepton pair annihilation and pair production in the hadron reactions is presently at the beginning stage. However, it will serve undoubtedly as one of the important tools in exploring both the dynamics and symmetry aspects of the ele-

mentary particle interactions.

ACKNOWLEDGEMENTS.

I am deeply grateful to my colleagues for clarifying discussions. The critical advices of Profs. A.M. Baldin and A.N. Tavkhelidze are gratefully acknowledged. I thank my wife for her patient help in preparing the manuscript.

R E F E R E N C E S

I) M.K. Moe, F. Reines. Phys. Rev., I40B, 992 (I965).

2) J.C. Zorn, G.E. Chamberlain, V.W. Hughes. Phys. Rev., I29, 2566 (I963).

3) I.Yu. Kobzarev, L.B. Okun. Uspekhi Fiz. Nauk, 95, I3I (I968).

A.S. Goldhaber, M.M. Nieto. Phys. Rev. Lett., 2I, 567 (I968).

4) D.A. Kirzhniz. Uspekhi Fiz. Nauk, 90, I29 (I966).

5) S.J. Brodsky, in Proc. of the 4-th Int. Symp. on Electron and Photon Interactions at High Energies, Liverpool, I969, p.3.

6) B.N. Taylor, W.H. Parker, D.N. Langenberg. Rev. Mod. Phys. 4I, 375(I969).

7) T. Appelquist, S. Brodsky. Phys. Rev. Lett., 24, 562(I970).

8) J. Gilleland, A. Rich. Phys. Rev. Lett., 23, II30 (I969).
J. Bailey et al. Phys. Lett., 28B, 287 (I968).

9) J. Aldins et al. Phys. Rev. Lett., 23, 44I (I969).

I0) F.E. Low. Phys. Rev., II0, 974 (I958).
S.L. Adler, Y. Dothan. Phys. Rev., I5I, I267 (I966).

II) For references on earlier papers see, S.B. Gerasimov, in Proc. of the Int. Seminar on Vector Mesons and Electromagnetic Interaction, Dubna, I969, p.367.

I2) G.C. Fox, D.Z. Freedman. Phys. Rev., I82, I628 (I969).

I3) Z.G.T. Guiragossian, in Proc. of the Int. Seminar on Vector Mesons and Electromagnetic Interactions, Dubna, I969, p.22I.

I4) S.B. Gerasimov. Dissertation, Dubna, I966.
T.P. Cheng, H. Pagels. Phys. Rev., I72, I635 (I968).

I5) R.L. Walker. Phys. Rev., I82, I729 (I969).

I6) C.A. Dominguez, C. Ferro Fontan, R. Suaya. Phys. Lett., 3IB, 365 (I970).

I7) M. Damashek, F.J. Gilman. SLAC-PUB-697, I969.

I8) J.J. Sakurai, in Proc. of the 4-th Int. Symp. on Electron and Photon Interactions at High Energies, Liverpool, I969, p.9I.

I9) A. Silverman, ibid., p.7I

20) L. Stodolsky. Phys. Rev. Lett., I8, I35 (I967).

2I) K. Gottfried, in Proc. of the Int. Seminar on Vector Mesons and Electromagnetic Interactions, Dubna, I969, p.I85.

22) H. Alvensleben, U. Becker et al., ibid., p.32I.

23) D. Schildknecht, ibid., p. I47.

24) D.S. Beder. Phys. Rev., I49, I203 (I966).

25) H. Harari, in Proc. of the 4-th Int. Symp. on Electron and Photon Interactions at High Energies, Liverpool, I969, p.I07.

26) R. Diebold, in Proc. of the Int. Conf. on High Energy Physics, Boulder, I969.

27) R.M. Ryndin, private communication

28) C.F. Cho, J.J. Sakurai. Phys. Lett., 30B, II9 (I969).

29) J.H. Scharenguivel et al. Phys. Rev. Lett., 24, 332(I970).

30) A.P. Contogouris et al. Phys. Rev. Lett., I9, I352 (I967)

31) L.J. Gutay et al. Phys. Rev. Lett., 22, 424 (1969).
R. Diebold, J.A. Poirier. Phys. Rev. Lett., 22, 255 (1969).

32) N.N. Biswas et al. Preprint of the University Notre Dame, 1969.

33) A.A. Logunov et al. Ann. Phys. (N.Y.) 31, 203(1965).

34) S.D. Drell, J.D. Walecka. Ann Phys. (N.Y.) 28, 18(1964).

35) L.N. Hand. Phys. Rev., 129, 1834 (1963).

36) W.K.H. Panofsky, in Proc. of the Int. Conf. on High Energy Physics, Vienna, 1968, p.23.

37) J.G. Rutherglen, in Proc. of the 4-th Int. Symp. on Electron and Photon Interactions at High Energies, Liverpool, 1969, p.163.

38) A.B. Clegg, ibid., p.123

39) R.E. Taylor, ibid., p.251

40) F. Gutbrot, ibid., p.141.

41) S.D. Drell et al. Phys. Rev., 157, 1402 (1967).

42) J.D. Bjorken, E.A. Paschos. Phys. Rev., 185, 1975 (1969).

43) H. Harari. Phys. Rev. Lett., 22, 1078(1969) , and 24, 286 (1970).

44) V.A. Matveev, R.M. Muradjan, A.N. Tavkhelidze. Preprint E2-4968, Dubna, 1970.

45) J.D. Bjorken. Phys. Rev. 148, 1467 (1966).
V.N. Gribov et al. Phys. Lett. 24B, 554 (1967).

46) T. Das et al. Phys. Rev. Lett., 19, 470 (1967).

47) J. Perez-y-Jorba, in Proc. of the 4 th Int. Symp. on Electron and Photon Interactions at High Energies, Liverpool, I969,p.2I3.
V.A. Sidorov, ibid., p.227.

48) C.W. Akerlof et al. Phys. Rev., I63, I482 (I967).

49) S. Coleman, H. Schnitzer. Phys. Rev. I34, B863 (I964).

50) N.M. Kroll, T.D. Lee, B. Zumino. Phys. Rev., I57, I376 (I967).

5I) J. Asbury et al. Phys. Lett., 25B, 565 (I967).

52) P.J. Biggs, D.W. Braben et al. Phys. Rev. Lett., 24, II97 (I970).

53) M.N. Khachaturjan, in Proc. of the Int. Conf. on Low and Intermediate Energy Electromagnetic Interactions, Dubna, I967, vol.I, p.53.

54) D. Bollini, A. Buhler-Broglin et al. Nuovo Cimento 56A, II73 (I968) and 57A, 404 (I968).

55) L. Lederman. Invited Talk at the 4 th Int. Symp. on Electron and Photon Interactions at High Energies, Liverpool, I969, see also Ref.I8.